# NRC/ANL INDUSTRY MEETING

Dated November, 6 2008

Argonne NATIONAL LABORATORY

... for a brighter future

# Tube-to-Tubesheet Joint Leakage

S. Majumdar, K. Kasza, C. Bahn, S. Bakhtiari and W. J. Shack

October 29-30, 2008

U.S. Department of Energy

UChicago Argonne LLC

A U.S. Department of Energy laboratory managed by UChicago Argonne, LLC

Work Sponsored by the US Nuclear Regulatory Commission

# Overview

- Material properties data
  - Alloy 600
  - A 508
- Structural and contact pressure analyses for severe accidents
  - Tube-to-collar junction test specimen
  - Model 51 tube-to-tubesheet junction.
- Leakage analysis for severe accident
  - Tube-to-collar specimen
  - Model 51 tube-to-tubesheet junction
- Leakage analysis for NO and MSLB

# Material Properties Data

- Key properties are the thermal expansion coefficients of A508 and Alloy 600
- We sent specimens of each material to ANTER Corp. and PMIC Corp.

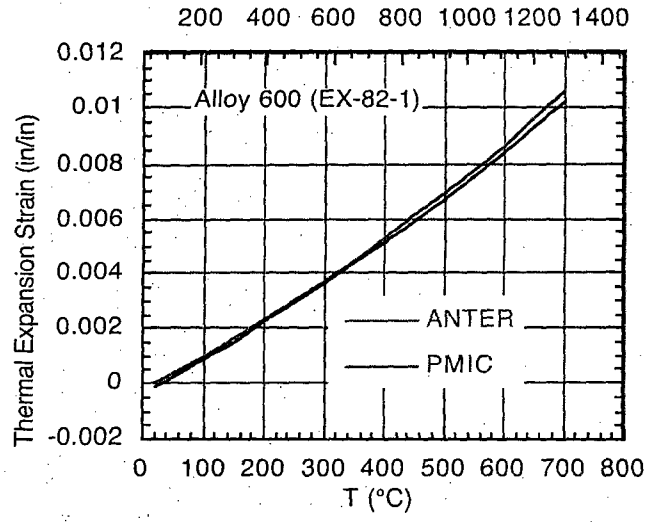


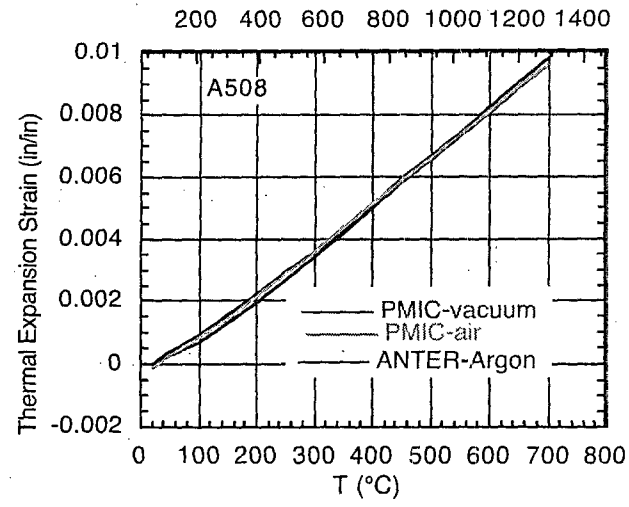


- The thermal expansion strains measured by both vendors are close.
- Fitted with 6$^{th}$ order polynomials

# Thermal Expansion Coefficient

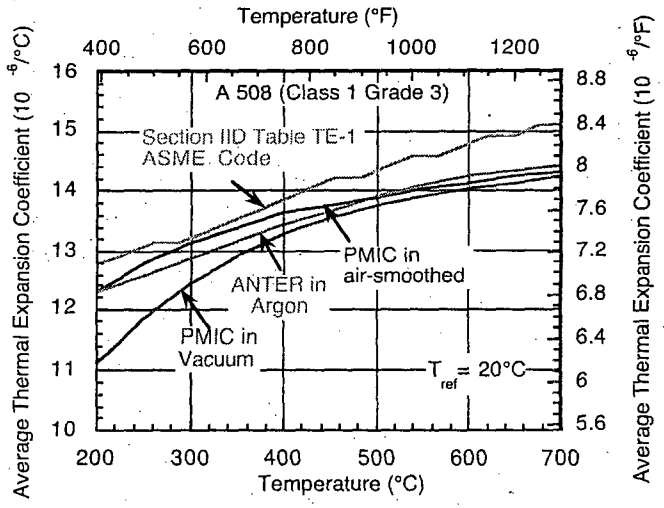


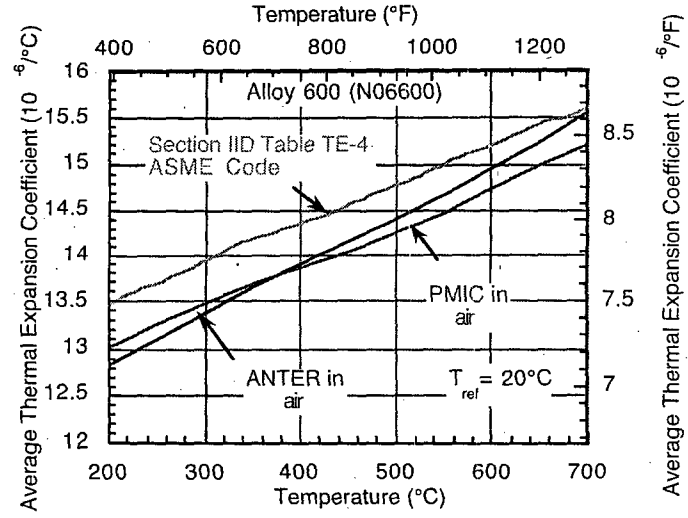

# B&W (Canada) Fit to PMIC Data of A508

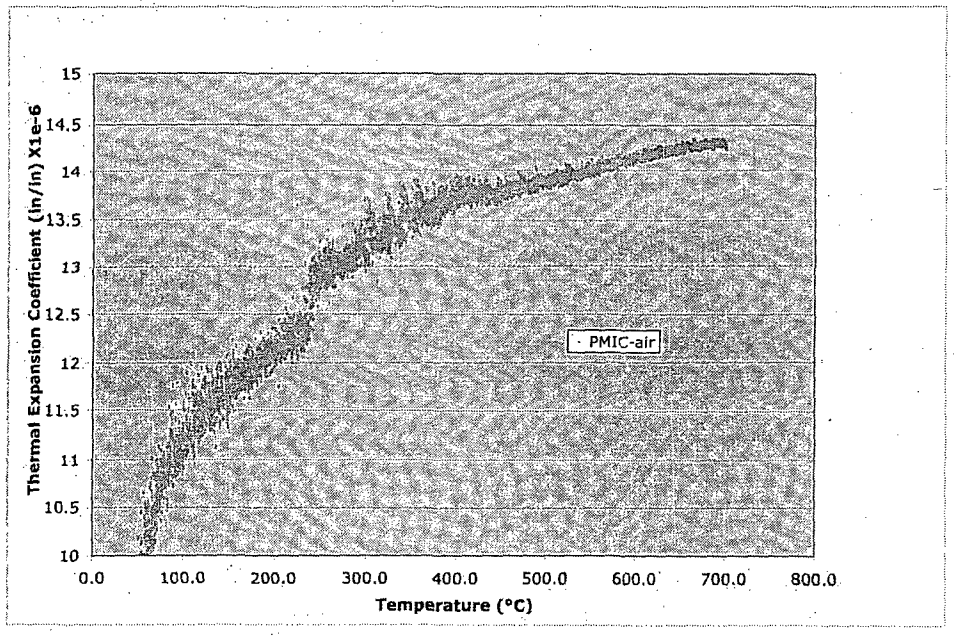


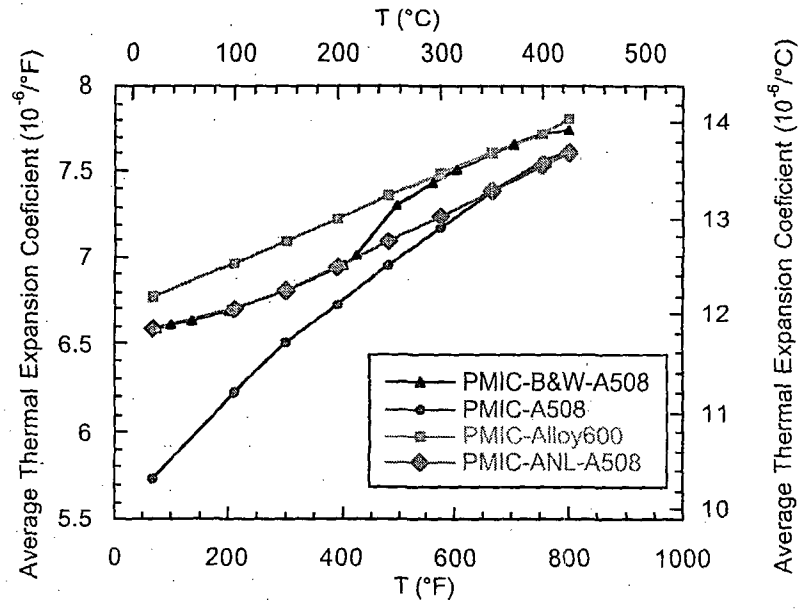


- The temperature region 250-350°C is important for analyzing NO and MSLB

# Mechanical Properties (Alloy 600 Tubes)

| Heat No. | Diam. in. (mm) | Yield ksi (MPa) | UTS ksi (MPa) | % Elongation |
|---|---|---|---|---|
| 8520L | 0.875 (22.2) | 42.5 (293) | 101 (696) | 36 |
| 8524 | 0.75 (19.05) | 44.7 (308) | 99 (682) | 25 |
| EX-82-1 | 0.875 (22.2) | 51.8 (357) | 99 (683) | 43 |

# Stress-Strain Curves at RT (Alloy 600)

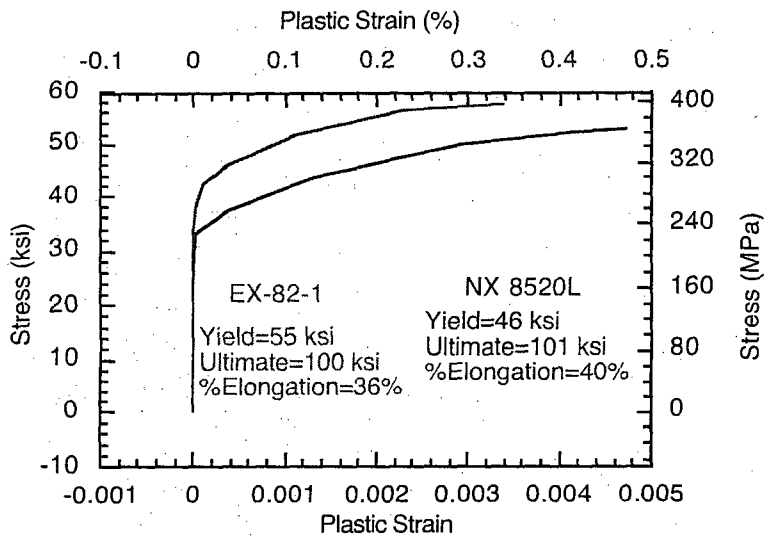


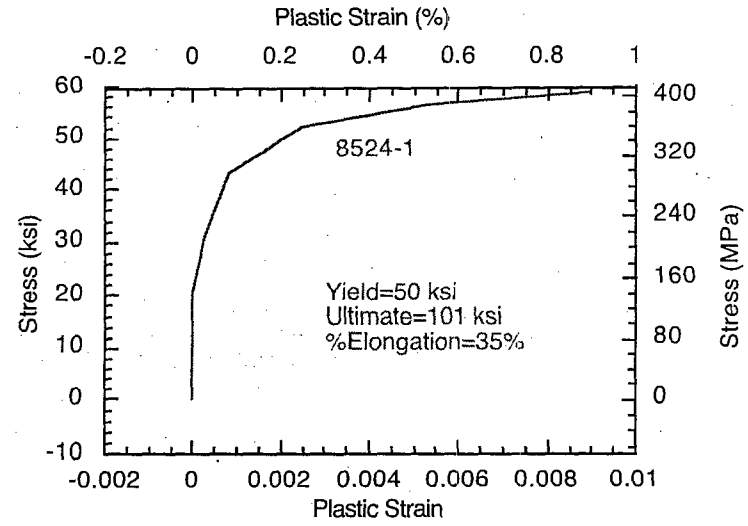


- NX 8524 properties are intermediate between those of the other two heats

# Mechanical Properties of A508 (Class 1 Grade 3)

- The SA 508 steel was obtained from a large forging.
- Following high temperature annealing, it was water quenched at 870°C (1600°F) for 11 h and tempered at 649°C (1200°F) for 15 h.

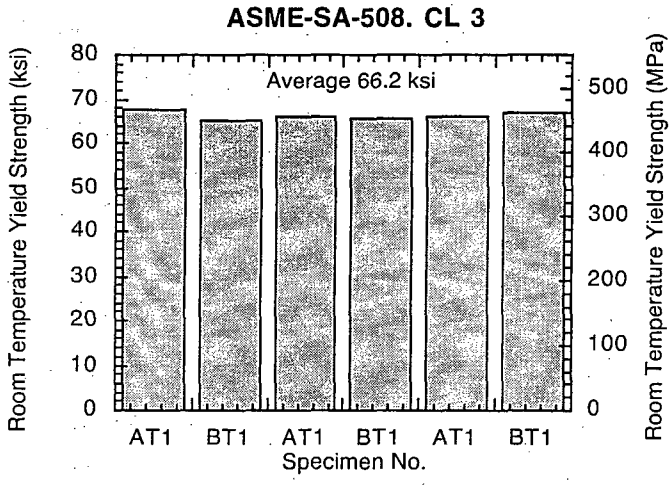


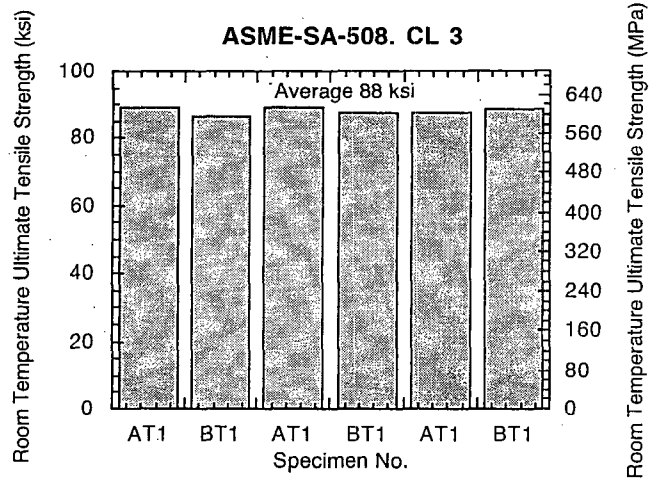


- Average yield of 66 ksi and average UTS of 88 ksi

# Stress-Strain Curves of A508 at RT

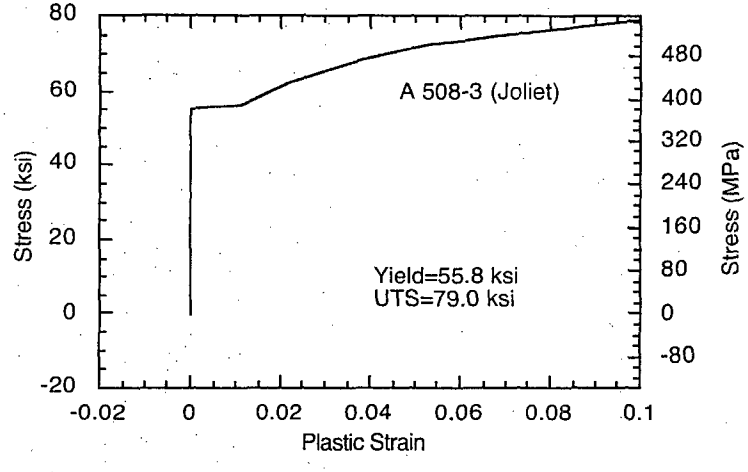


4-hr/1125°F PWHT

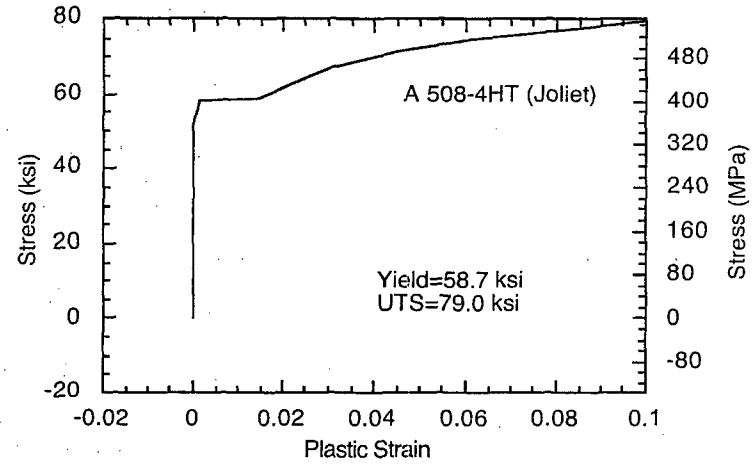


3-hr/1125°F PWHT

- PWHT appears to have softened the material significantly
- The extra 1-hr PWHT was applied to facilitate machining of our tube-to-collar specimens

# Stress-Strain Curves at High temperatures

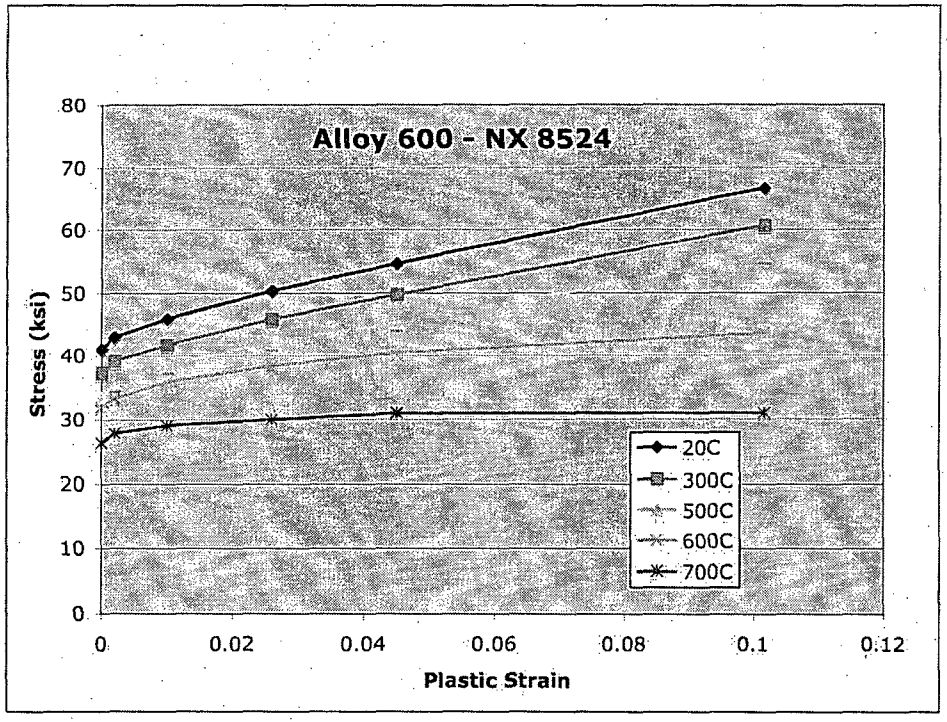


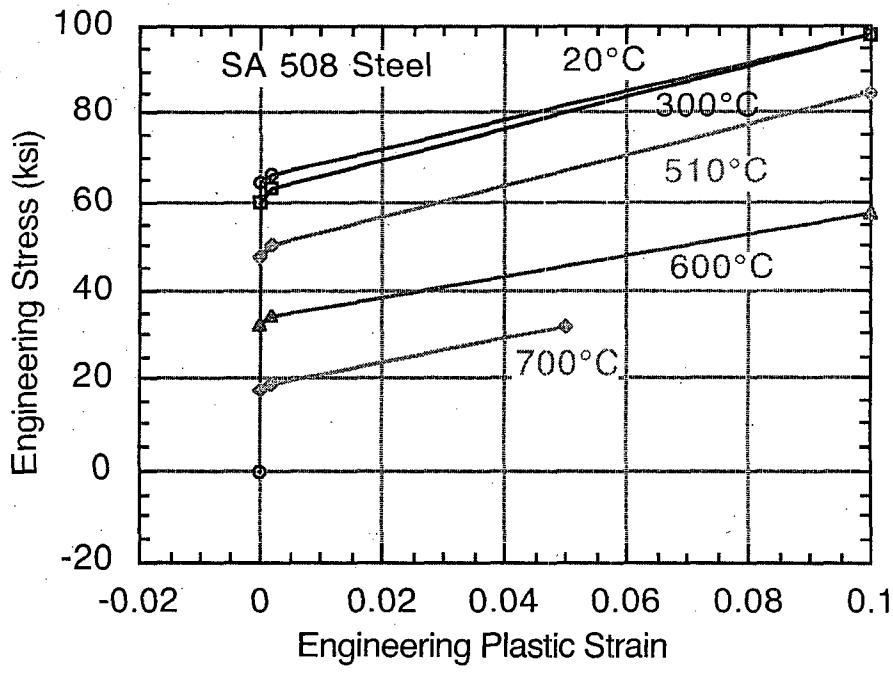

# Creep Rate Equations

$$\varepsilon_c = \varepsilon_{c,p} + \varepsilon_{c,s}$$

$$\varepsilon_{c,p} = A_1 \sigma^{n1} \exp\left(-\frac{Q_1}{T}\right)\left[1 - \exp\left(-\frac{t}{t_0}\right)\right]$$

$$\varepsilon_{c,s} = A_2 t \sigma^{n2} \exp\left(-\frac{Q_2}{T}\right)$$

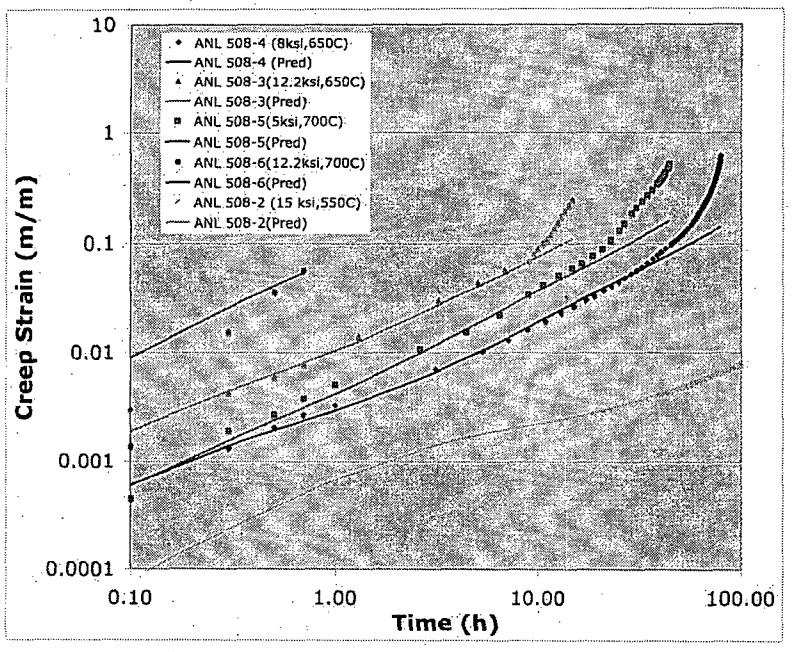

# *Design of Tube-to-Collar Test Specimens*

- We designed the collar such that its radial elastic stiffness is the same as that of the tubesheet.
- First, calculated the orthotropic elastic constants of the tubesheet material

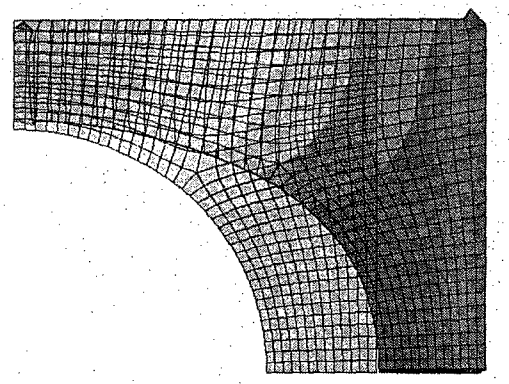

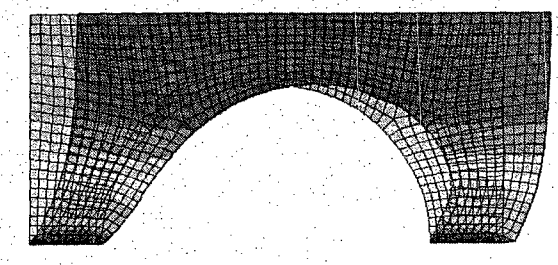

- 1.28 in. pitch and 0.891 in. tube hole diameter for 0.875 in. diameter SG tubes arranged in a square array in tubesheet (50"radius, 21" thick)
- Applied unit normal and shear strains to a unit cell of the tubesheet
- Applied unit pressure at the tube hole in a tubesheet
- Applied unit pressure on the ID surface of the collar
- Determined radial thickness of the collar by equating the radial stiffnesses.

# *Finite Element Model of Tube-to-Collar Specimen*

- Axisymmetric model (initial radial clearance of 0.008") including the tack region
- Axisymmetric solid elements for both tube and collar
- Surface-to-surface contact ($\mu$=0.2) between tube OD and collar ID
- Seal weld at the bottom modeled by constraining the axial displacements of the tube and the collar to be the same
- Rigid body translation in the axial direction prevented by applying displacement boundary condition at the OD point at the bottom of the collar.
- Pressure loading only (isothermal)

# Finite Element Model of ANL Test Specimen

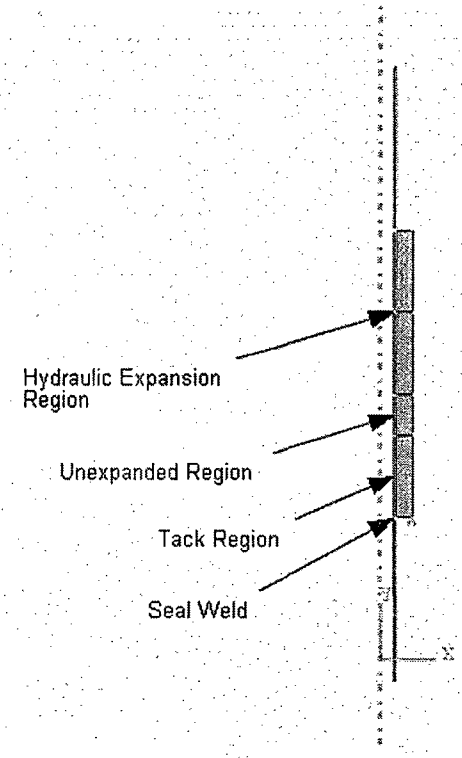

# *Finite Element Analysis of Tube-to-Collar Specimen*

- Step 1 Tack expansion and Hydraulic expansion pressures applied and removed
- Step 2 Tube internal pressure applied
- Step 3 Temperature of the specimen raised

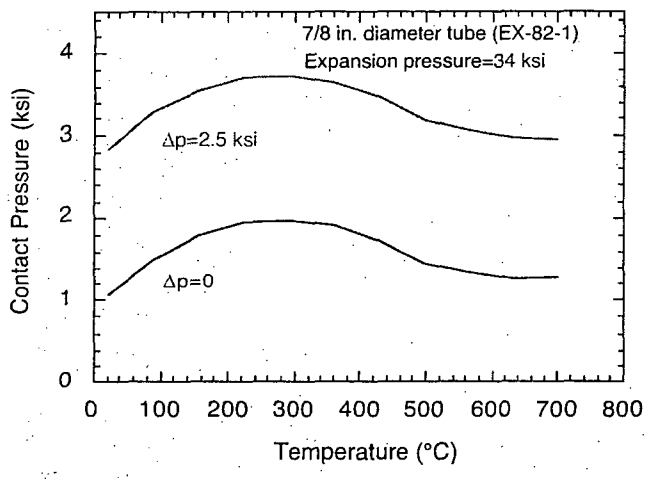


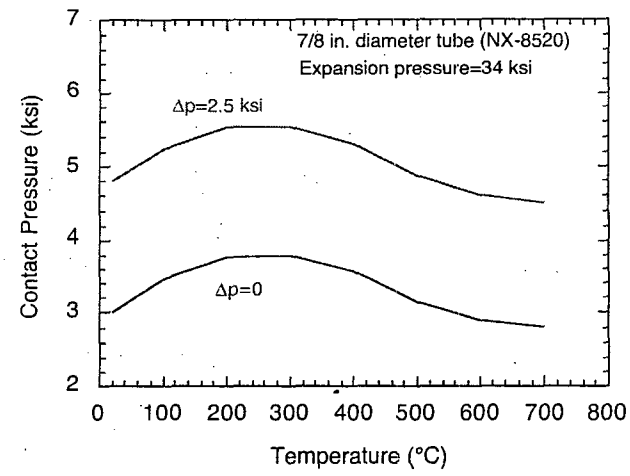


- Thermal stress depends on the differential thermal expansion coefficient
- Initial contact pressure is higher the lower the yield strength

# Leakage During Screening Tests at RT

| Specimen # (Heat #) | Leak Rate[a] (mg/min) | | | Leak Path Length in. (mm) | Initial contact pressure ksi (MPa) |
|---|---|---|---|---|---|
| | 0.5 ksi (3.5 MPa) | 1 ksi (6.9 MPa) | 1 ksi (6.9 MPa) | | |
| #01-3/4 (NX8524) | 0.5 | 3.5 | 4.3 | 4 (100) | 3 (21) |
| #04-7/8 (NX8520 LT) | 0.8 | 2.7 | 2.7 | 4 (100) | 3 (21) |
| #05-7/8 (EX-82-1) | No Leak | 24.3 | 23.8 | 4 (100) | 1 (7) |

- Leak rates are consistent with calculated contact pressure
- Significant scatter in the data

# Effect of Thermal Ramp to 300°C on Leak Rate

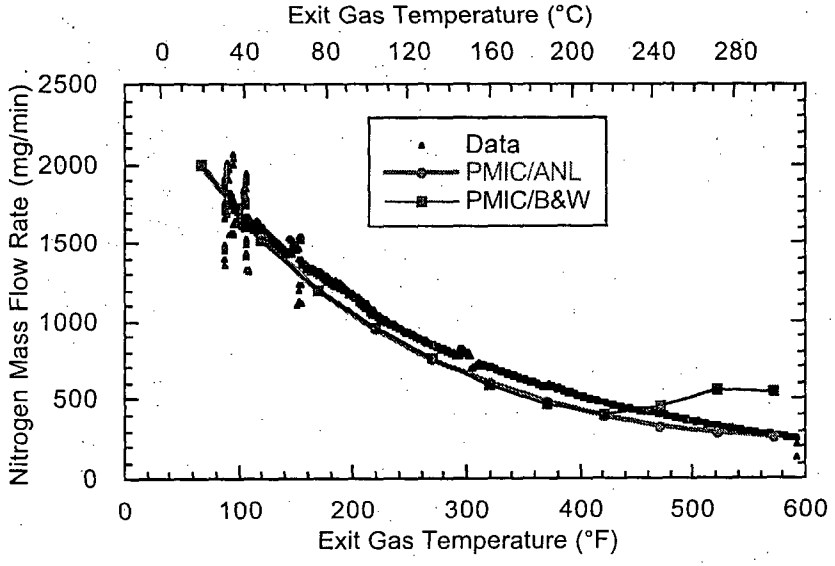


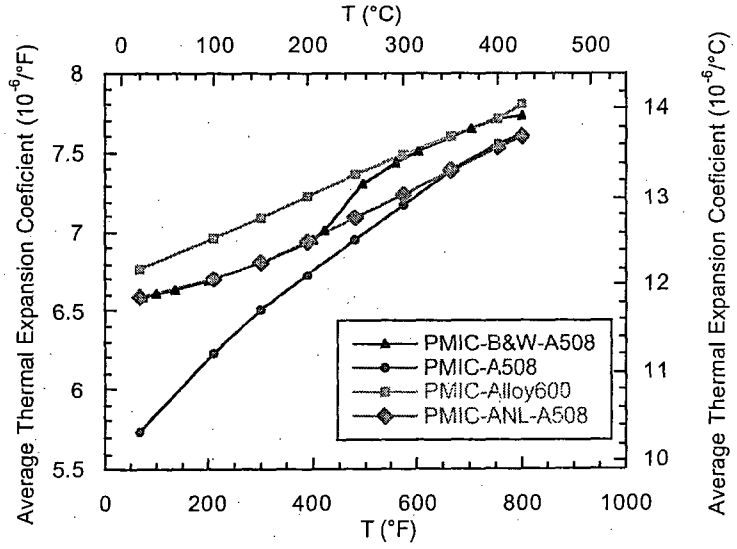


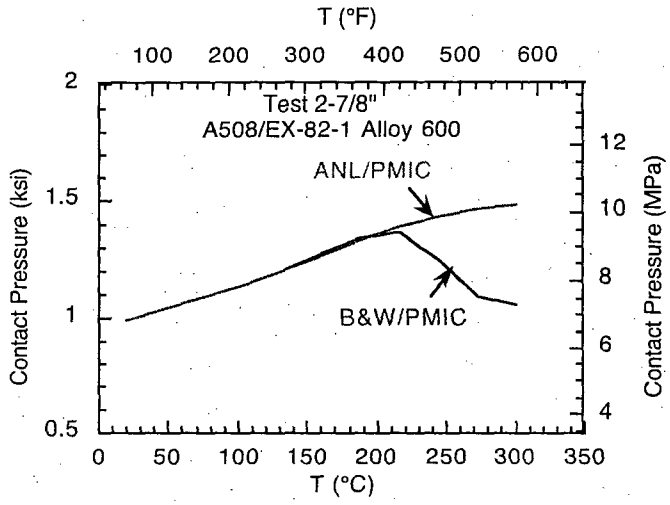


- The upward jog in the thermal expansion coefficient proposed by B&W is not consistent with leak rate data (Test 2-7/8")

# Analysis of Contact Pressure (7/8"Tube)

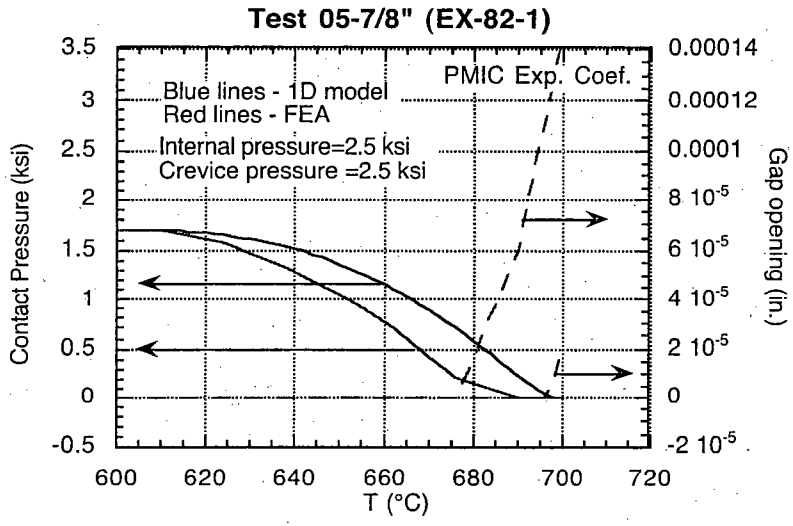


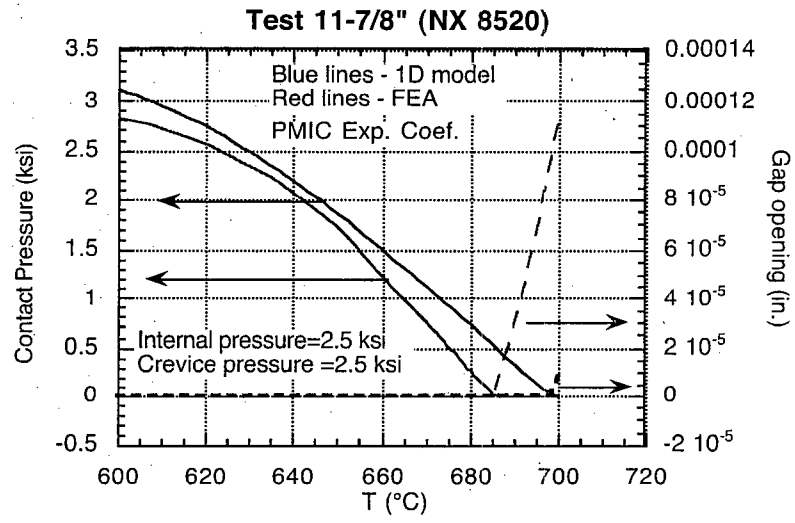


- Contact pressure reduces to zero at 680°C for EX-82-1 and 690°C for NX 8520.
- These temperatures are close to the test temperatures at which large leakages were observed.

# Model 51 Tubesheet Model

- Tubesheet with holes replaced by equivalent tubesheet with effective orthotropic thermal and mechanical properties.

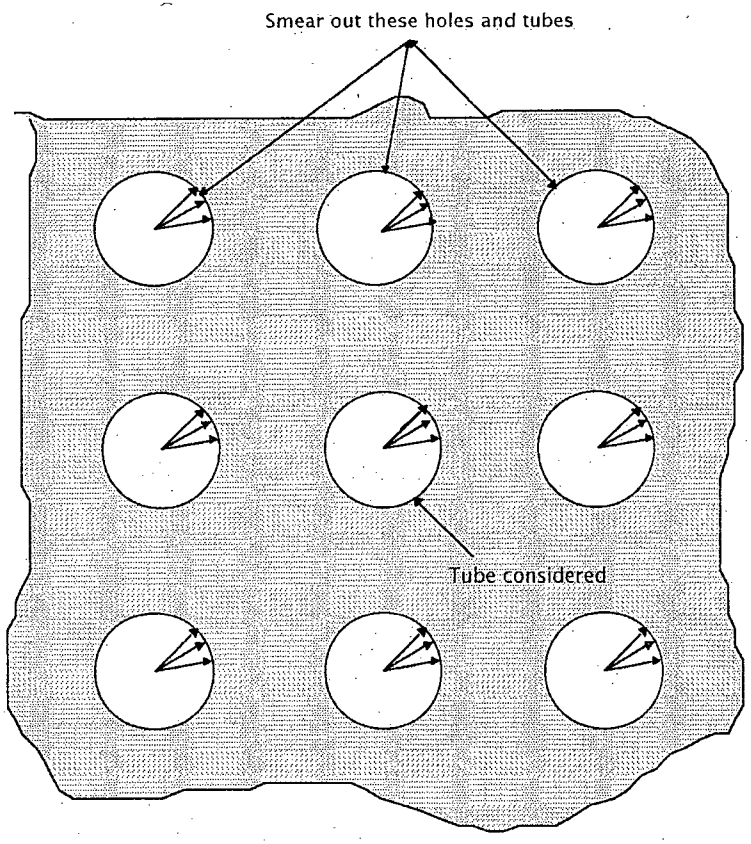


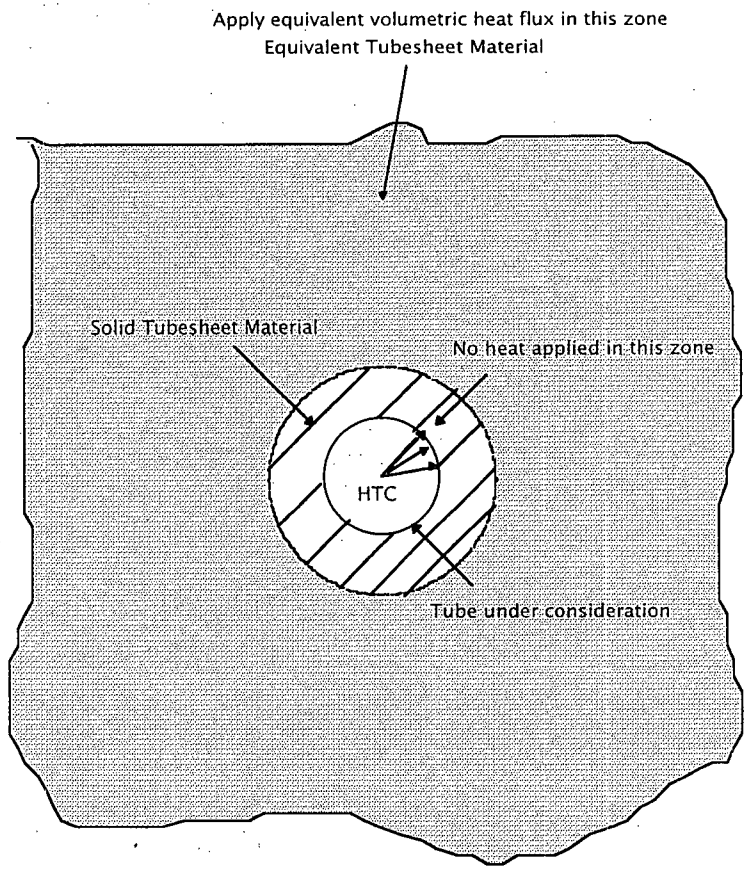

# Determination of Effective Uniaxial Yield Properties

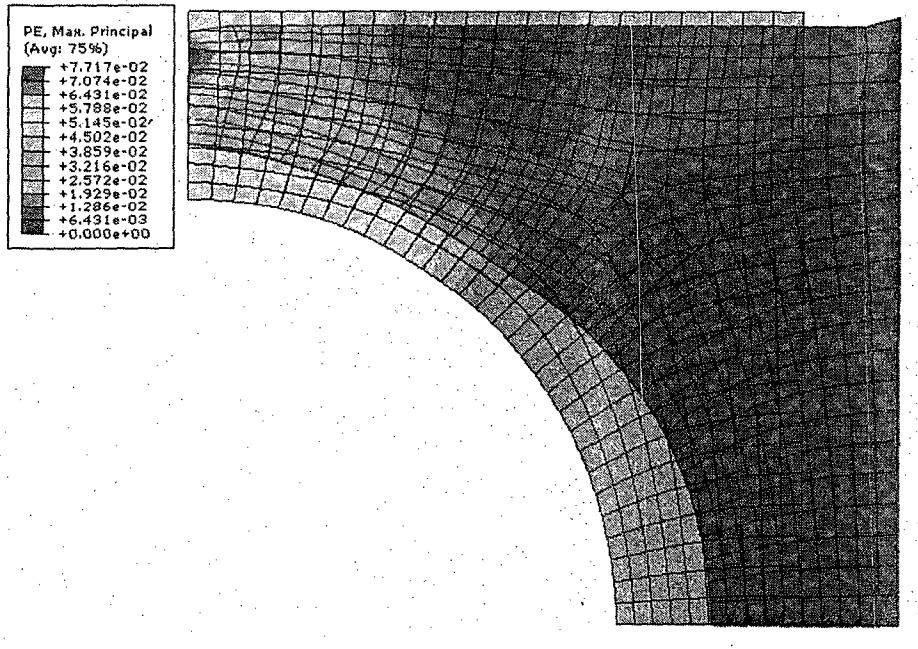


- Apply X-displacement to unit cell
- Apply zero Y and Z displacements to remove rigid body translations
- Use X, Y and Z symmetry
- Couple Y and Z displacements on appropriate faces
- No net load in Y and Z direction
- Compute X-load vs. displacement

# Results for X-Displacement

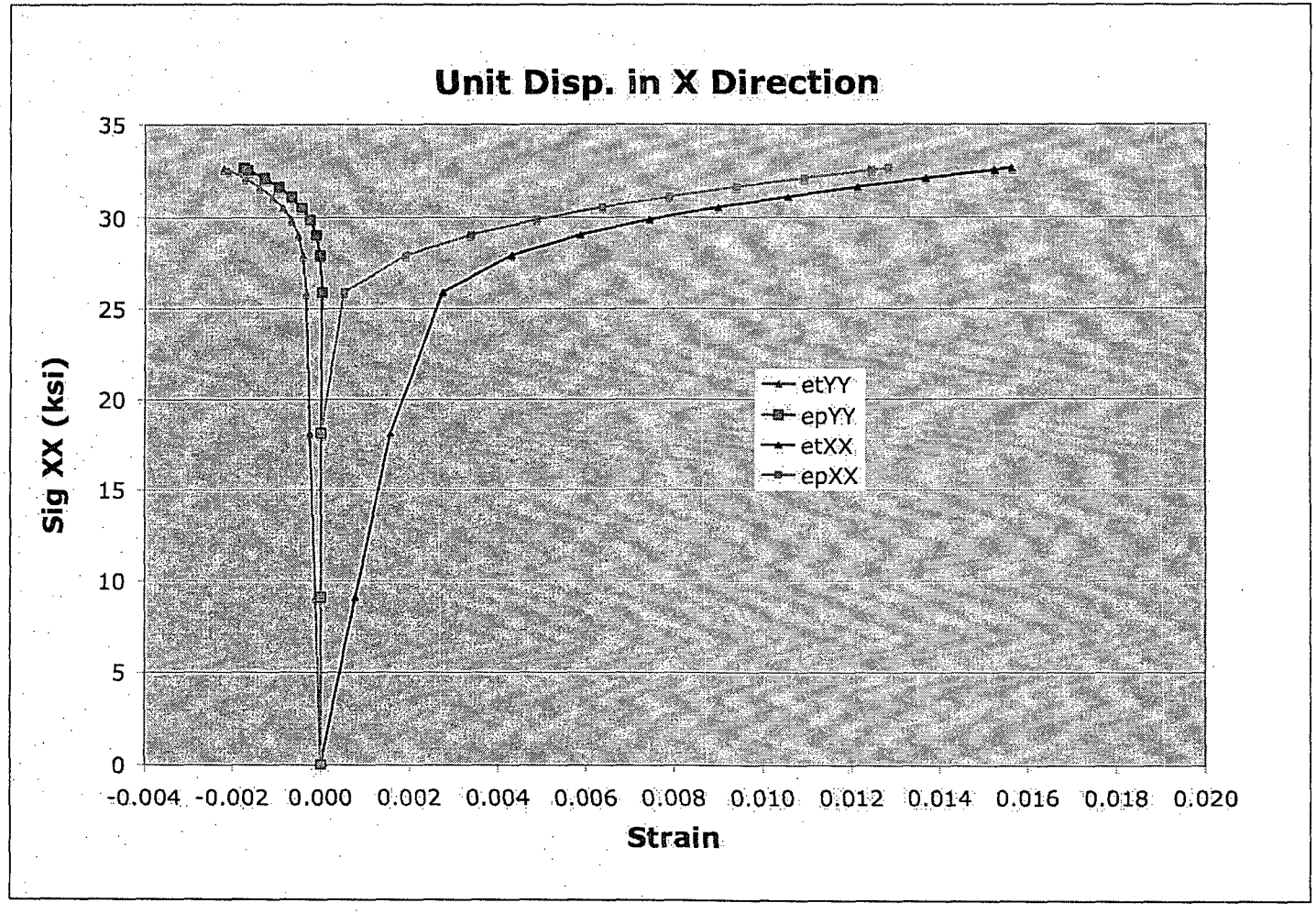

# Determination of Effective Shear Yield Properties

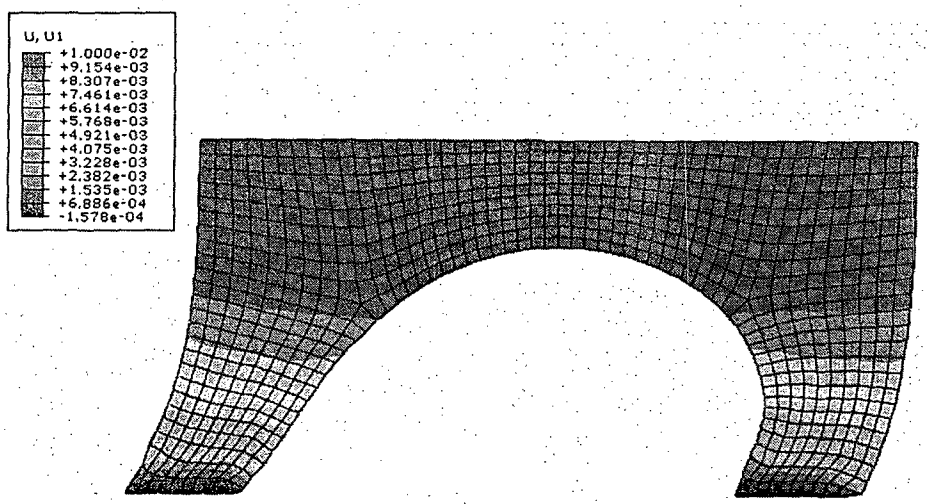


- Apply X-shear displacement to unit cell
- Apply zero X, Y and Z displacements to remove rigid body translations
- Couple Y and Z displacements on appropriate faces
- No net load in Y and Z direction
- Compute X-load vs. displacement

# Hill's Formulation for Anisotropic Plasticity

$$f(\sigma)=\sqrt{\left[F(\sigma_r-\sigma_\theta)^2+G(\sigma_z-\sigma_r)^2+H(\sigma_\theta-\sigma_z)^2+2L\sigma_{r\theta}{}^2+2M\sigma_{rz}{}^2+2N\sigma_{z\theta}{}^2\right]}$$

where

$$F=\frac{\left(\sigma^0\right)^2}{2}\left[\frac{1}{\sigma_{r,y}^2}+\frac{1}{\sigma_{\theta,y}^2}-\frac{1}{\sigma_{z,y}^2}\right]=\frac{1}{2}\left[\frac{1}{R_{11}^2}+\frac{1}{R_{33}^2}-\frac{1}{R_{22}^2}\right],$$

$$G=\frac{\left(\sigma^0\right)^2}{2}\left[\frac{1}{\sigma_{r,y}^2}+\frac{1}{\sigma_{z,y}^2}-\frac{1}{\sigma_{\theta,y}^2}\right]=\frac{1}{2}\left[\frac{1}{R_{11}{}^2}+\frac{1}{R_{22}{}^2}-\frac{1}{R_{33}{}^2}\right],$$

$$H=\frac{\left(\sigma^0\right)^2}{2}\left[\frac{1}{\sigma_{z,y}^2}+\frac{1}{\sigma_{\theta,y}^2}-\frac{1}{\sigma_{r,y}^2}\right]=\frac{1}{2}\left[\frac{1}{R_{22}{}^2}+\frac{1}{R_{33}{}^2}-\frac{1}{R_{11}{}^2}\right],$$

$$L=\frac{3}{2}\left(\frac{\tau^0}{\sigma_{r\theta,y}}\right)^2=\frac{3}{2R_{13}{}^2},\ M=\frac{3}{2}\left(\frac{\tau^0}{\sigma_{rz,y}}\right)^2=\frac{3}{2R_{12}{}^2},\ \text{and}\ N=\frac{3}{2}\left(\frac{\tau^0}{\sigma_{z\theta,y}}\right)^2=\frac{3}{2R_{23}{}^2}$$

# Effective Stress-Strain Curves for Tubesheet

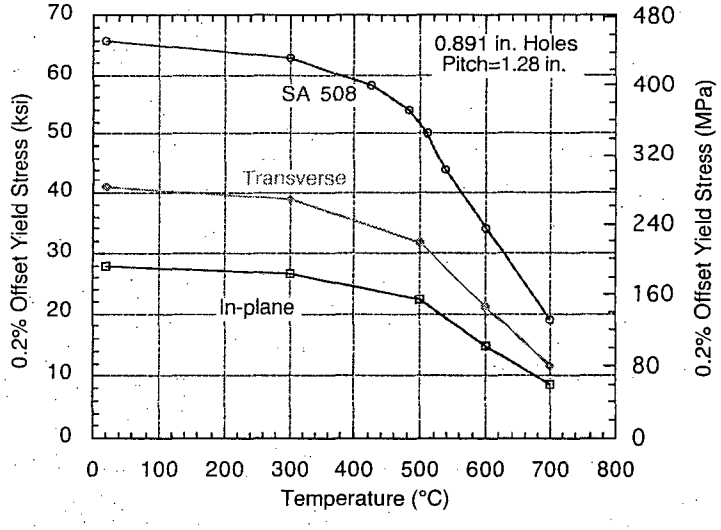


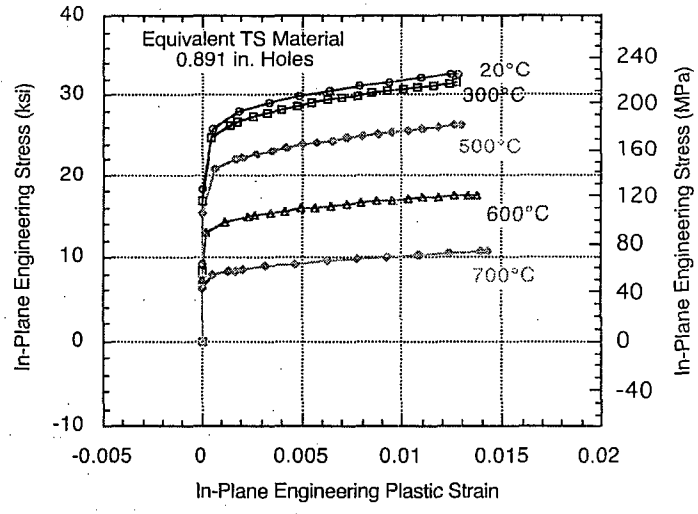

# Effective Creep Properties of Tubesheet

- Effective anisotropic properties (Hill's formulation) determined from FEA of unit cells.

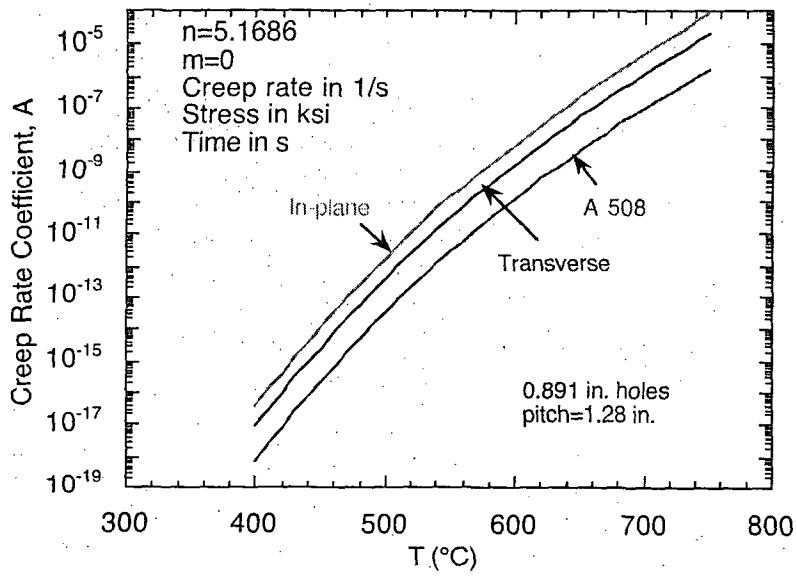


- Available literature creep rate data for A508 steel at high temperatures were fitted to the following equation:

$$\dot{\varepsilon}_c = B\exp\left(-\frac{Q}{T}\right)\sigma^n t^m, \quad A = B\exp\left(-\frac{Q}{T}\right)$$

# Determination of Equivalent Bulk Heating Rates

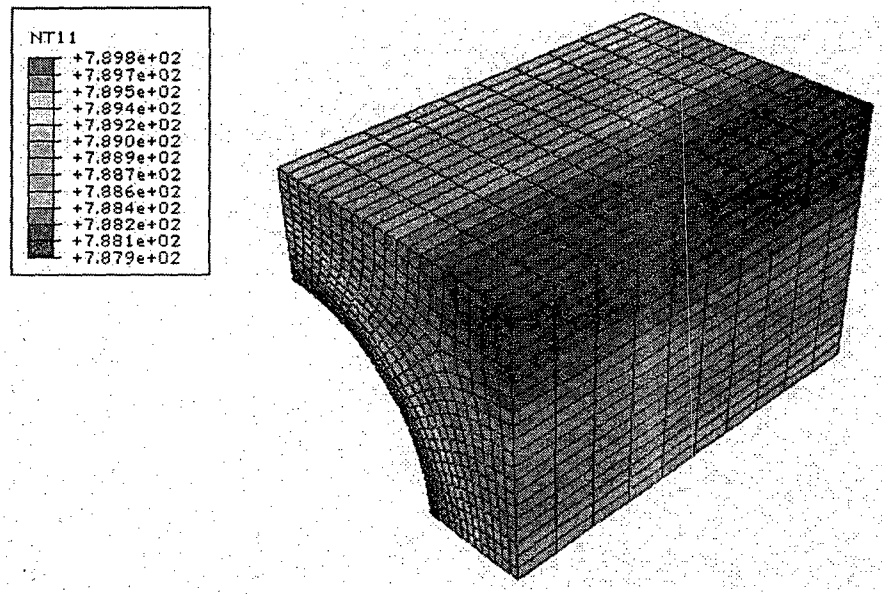


Unit cell

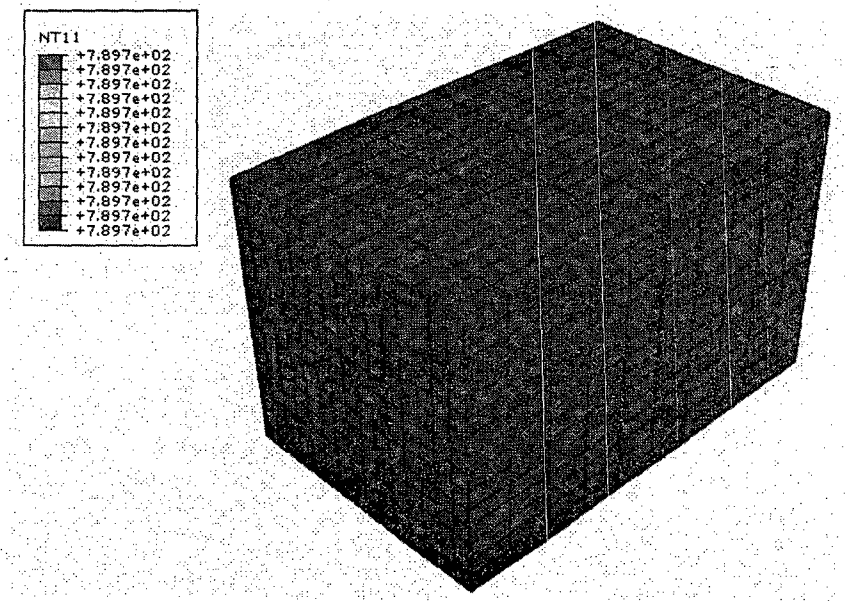


Equivalent material

- Unit cell subjected to HTC and Tgas from RELAP5
- Equivalent material subjected to uniform bulk heating
- Determined effective anisotropic thermal conductivities

# *Thermal Analysis Inputs (SBO Severe Accident Base Case)*

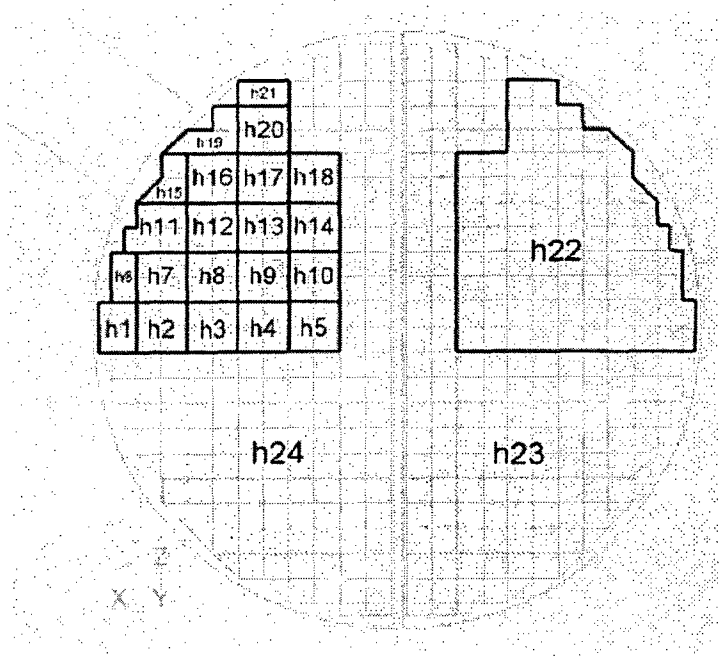


- HTC and Tgas for hot inlet (h1-h21) provided by Boyd based on CFD analysis.
- We used Cell 16 data as representative of hot tubes
- Equivalent bulk heating rate based on RELAP 5 calculated data (ISL) used for hot outlet (cell 22), cold outlet (cell 23) and cold inlet (cell 24).

# Finite Element Model

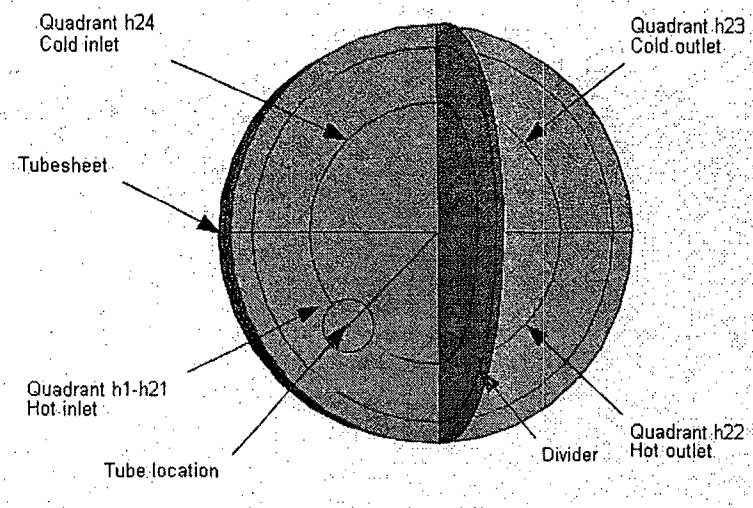


- FEM included a single tube, tubesheet (with solid rim), divider plate, lower head and a SG shell segment.

# Thermal Analysis Results

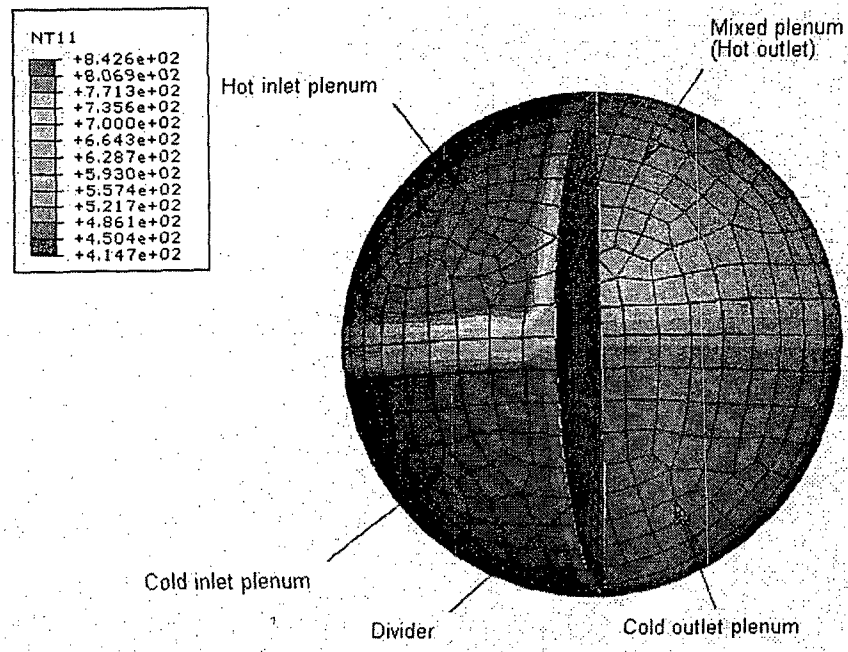


Lower head (ID surface) t=13,750 s

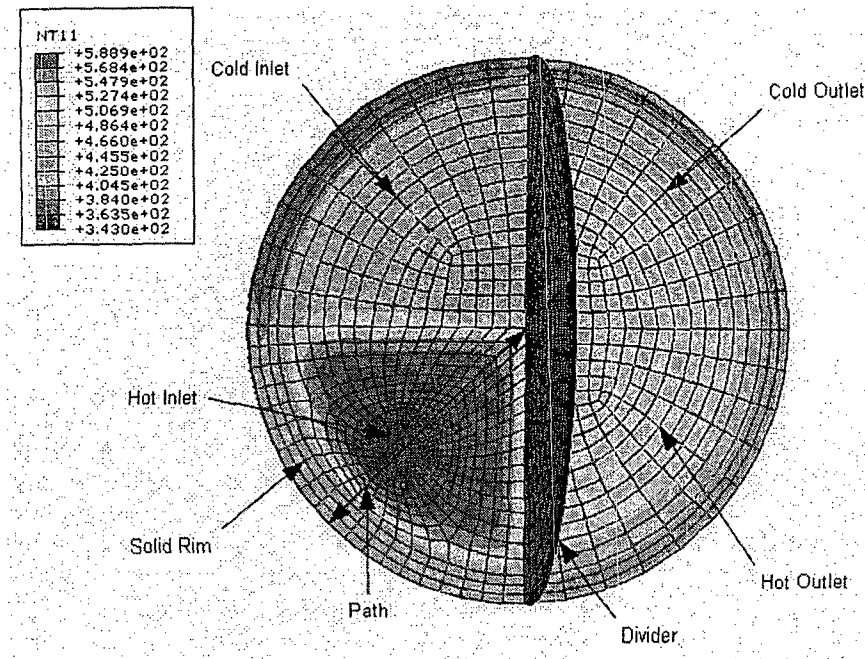


(TS bottom surface) t=12420 s

# Temperature Distribution in the Tube and Tubesheet

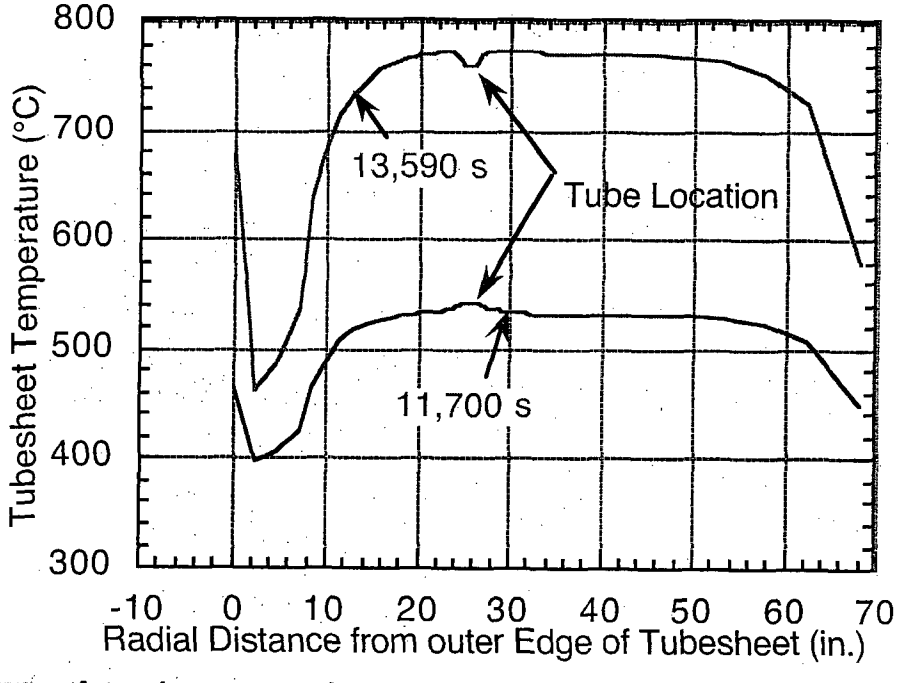


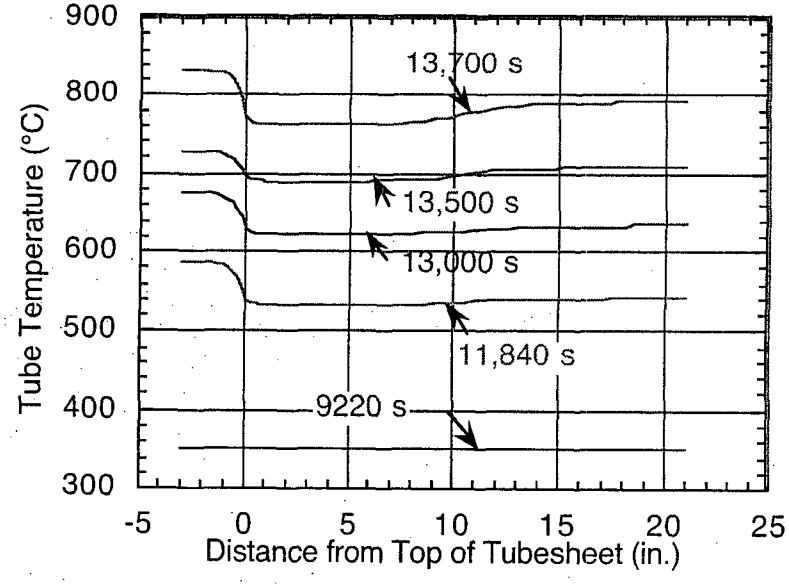


- At shorter times, tube is hotter than the surrounding
- Exposed tube is hotter than the tube within the tubesheet.

# Contact Pressure Analysis Results

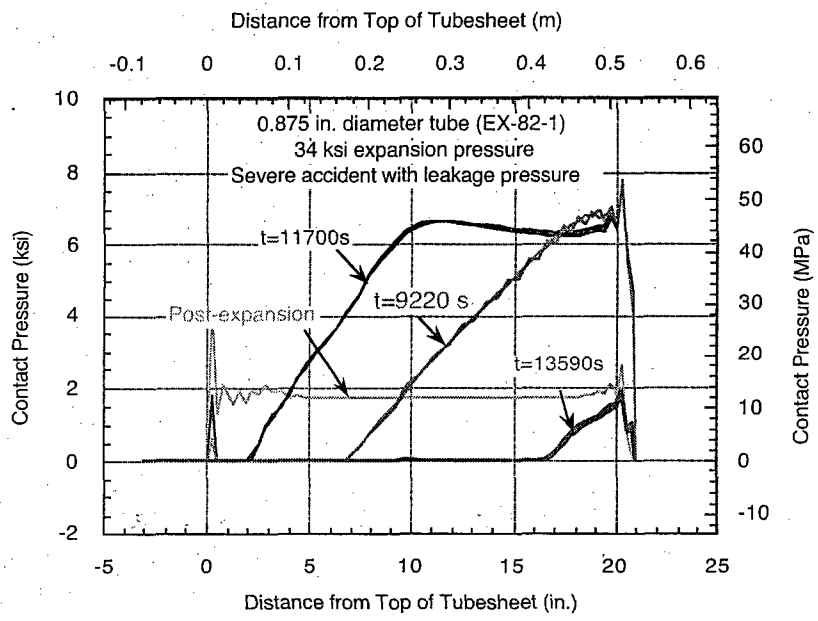


with crevice pressure

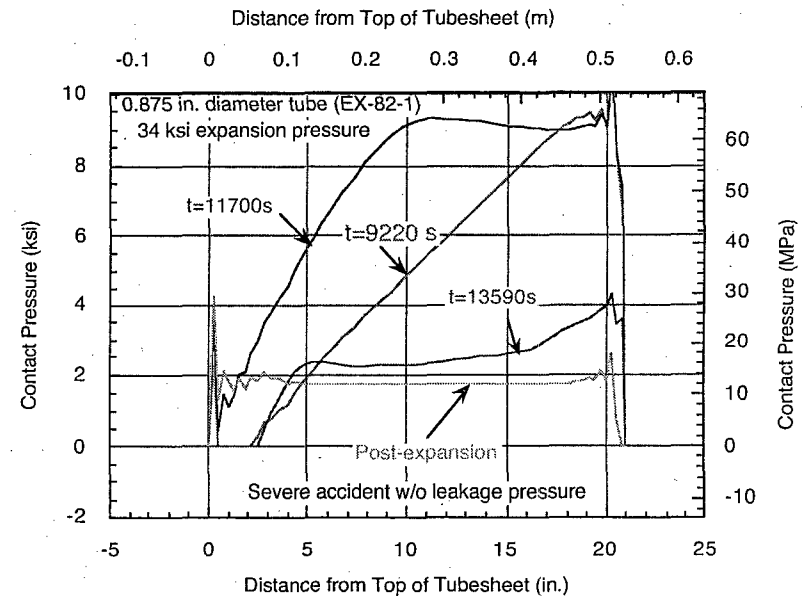


w/o crevice pressure

- Large leakage unlikely without crevice pressurization

# *Tubesheet Deformation Effect*

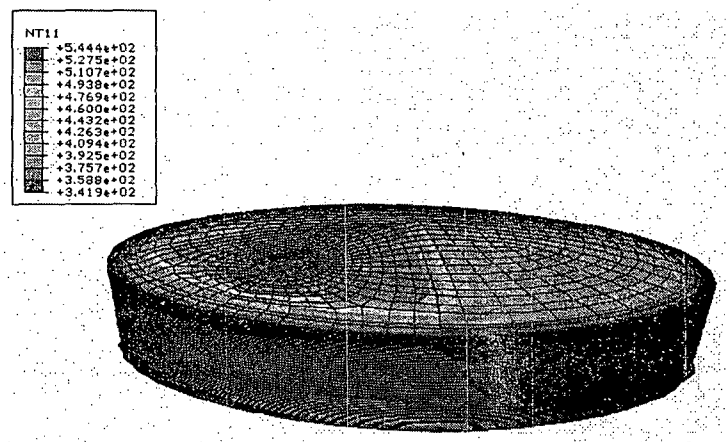


t=11,700s

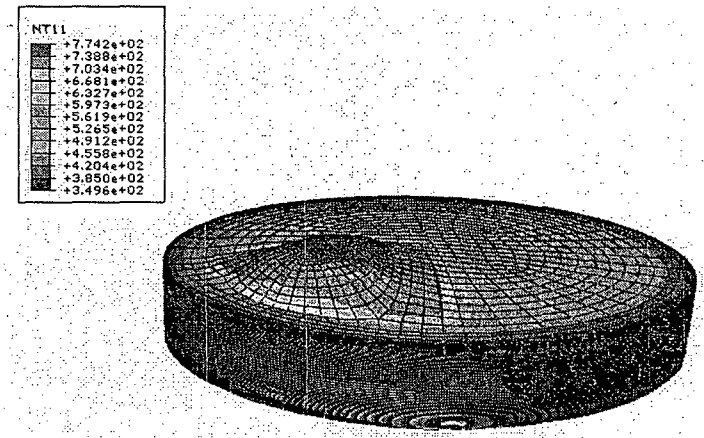


t=13,590s

- At lower temperatures bowing is approximately axisymmetric
- At higher temperatures, additional local bending due to creep.
  - Causes non-axisymmetric contact pressure distribution in the tube

# Circumferential Contact Pressure and Gap Variations (Uniform Crevice Pressure Dist.)

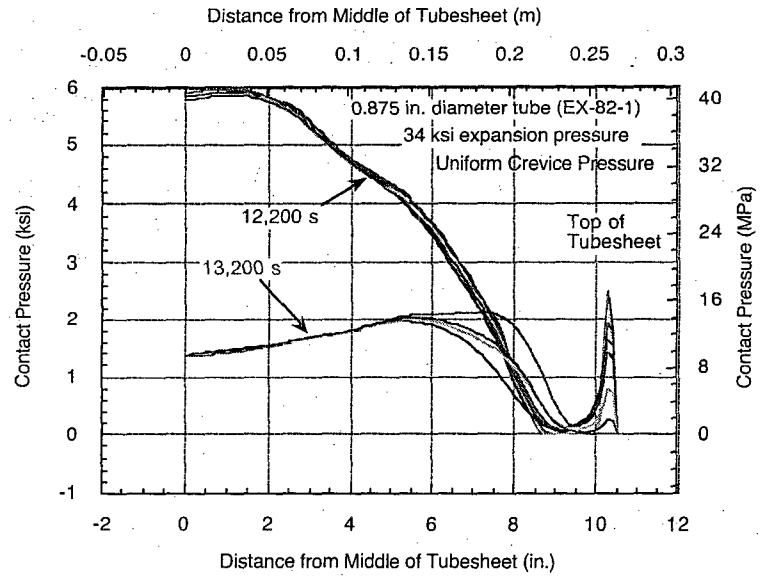


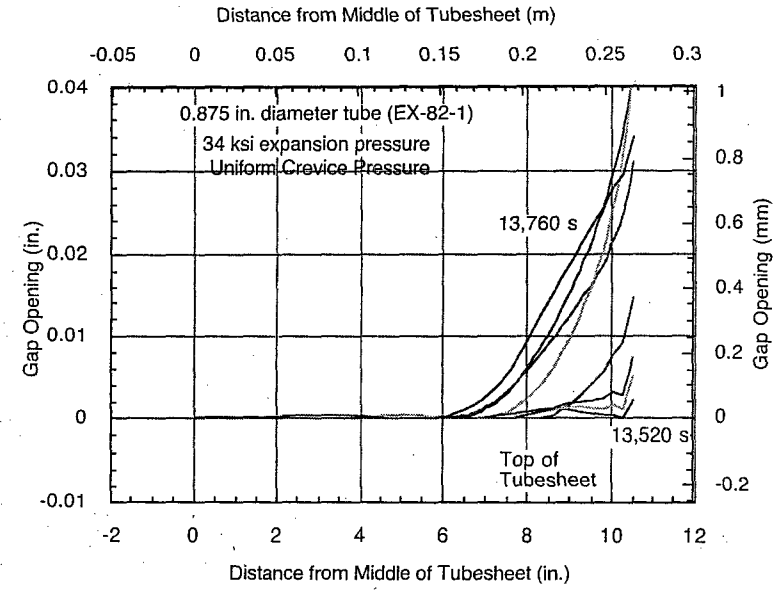


- Four axial paths separated from each other by 90° in the circumferential direction
- Throughwall crack assumed to be at TS mid-thickness

# Circumferential Contact Pressure and Gap Variations (Parabolic Crevice Pressure Dist.)

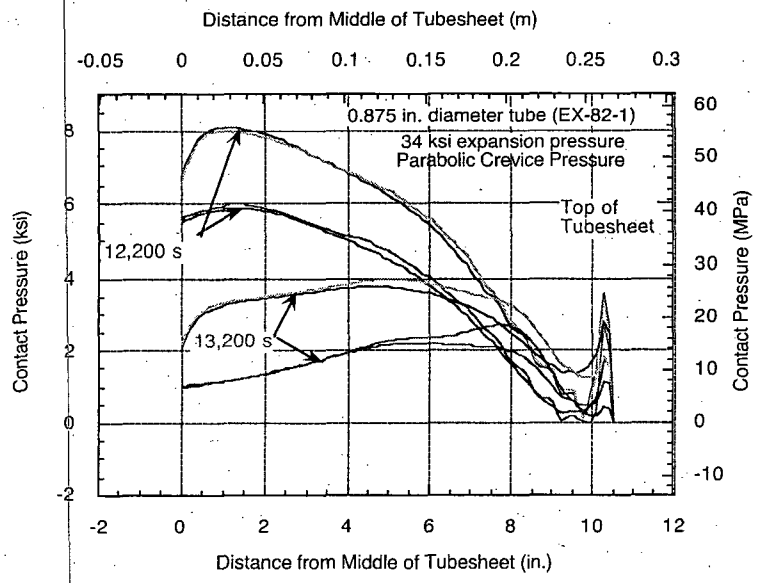


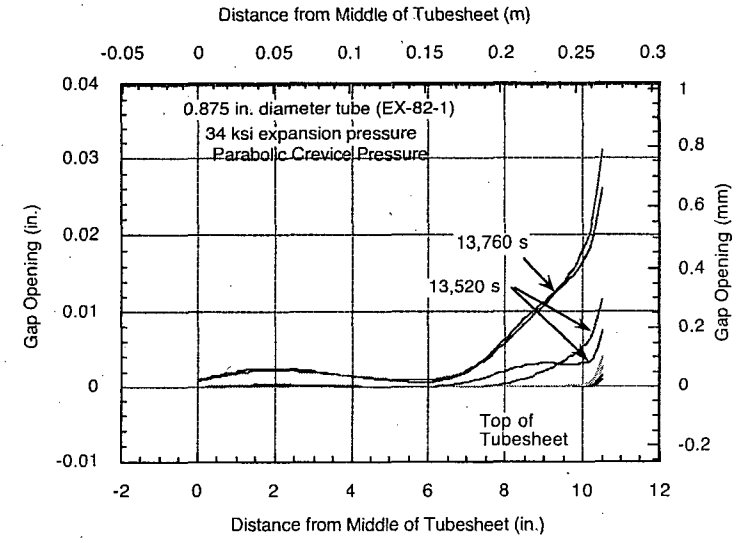


- Four axial paths separated from each other by 90° in the circumferential direction
- Significant circumferential variation – leak rate model assumes axisymmetric contact pressure and gap opening with no circumferential flow
- Non-axisymmetry implies that the flow will be circumferential from high resistance to low resistance before turning axial.

# Ring Assembly Model for Leak Rate

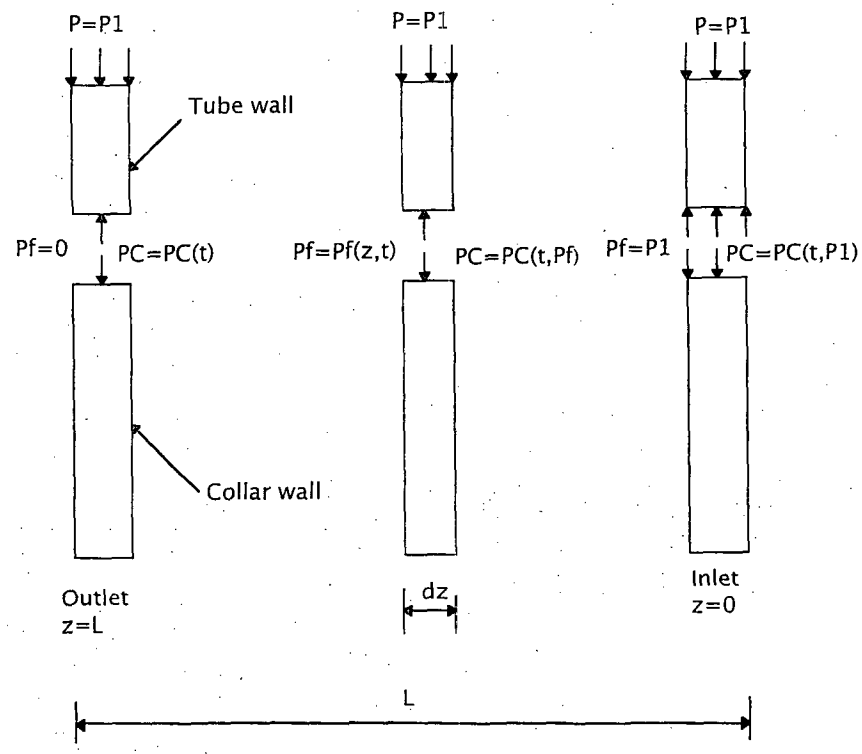


$$q\int_0^L dz = -\frac{\rho_1}{\mu}\int_{p_1}^{p_2}\left(\rho(p_f)\big/K\rho(p_1)\right)dp_f = \frac{-1}{v_1}\int_{p_1}^{p_2}\left(p_f\big/Kp_1\right)dp_f$$

# Effective Gap Width

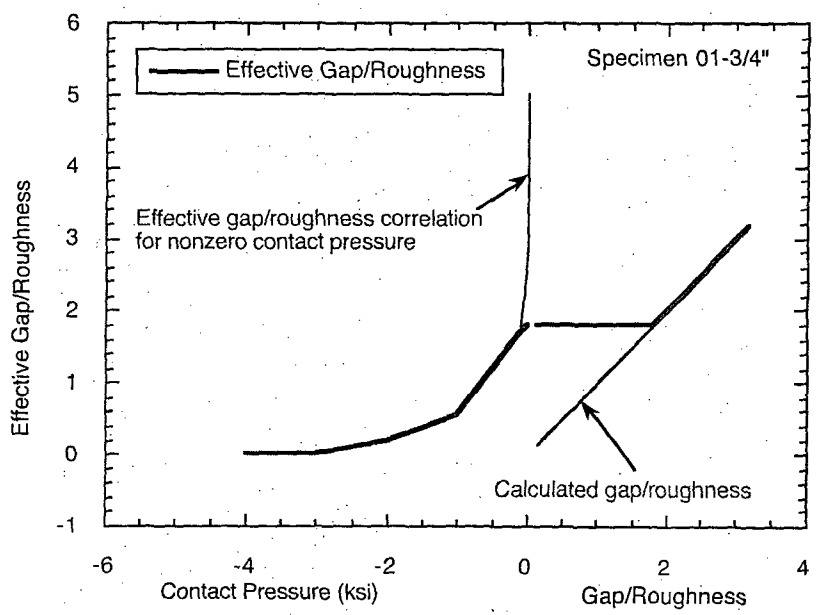


- Bold line used as normalized effective gap width

# Leakage Analysis Steps (Ring Assembly Model)

| TIME | TEMPERATURE | PTUBE | PCREVICE | PCONTACT | GAP | $h_{corr}$ | K |
|---|---|---|---|---|---|---|---|
| 14402 | 710 | 2.5 | 0 | 2.13 | 0.00E+00 | 5.65E-05 | 6.65E+13 |
| 14402 | 710 | 2.5 | 0.25 | 1.88 | 0.00E+00 | 6.87E-05 | 3.69E+13 |
| 14402 | 710 | 2.5 | 0.5 | 1.65 | 0.00E+00 | 8.16E-05 | 2.20E+13 |
| 14402 | 710 | 2.5 | 0.75 | 1.40 | 0.00E+00 | 9.78E-05 | 1.28E+13 |
| 14402 | 710 | 2.5 | 1 | 1.14 | 0.00E+00 | 0.000117 | 7.36E+12 |
| 14402 | 710 | 2.5 | 1.25 | 0.69 | 0.00E+00 | 0.000167 | 2.58E+12 |
| 14402 | 710 | 2.5 | 1.5 | 0.34 | 0.00E+00 | 0.000237 | 8.97E+11 |
| 14402 | 710 | 2.5 | 1.75 | 0.024 | 0.00E+00 | 0.000393 | 1.96E+11 |
| 14402 | 710 | 2.5 | 2 | 0 | 4.96E-05 | 0.000393 | 1.96E+11 |
| 14402 | 710 | 2.5 | 2.25 | 0 | 1.21E-04 | 0.000393 | 1.96E+11 |
| 14402 | 710 | 2.5 | 2.5 | 0 | 2.27E-04 | 0.000393 | 1.96E+11 |

$$q = -\frac{v_1}{L}\int_{p_1}^{0}\frac{\left(p_f/p_1\right)}{K}dp_f \qquad z = -\frac{v_1}{q}\int_{p_1}^{p_f}\frac{\left(p_f/p_1\right)}{K}dp_f$$

# Crevice Gas Pressure Distribution (Ring Assembly Model)

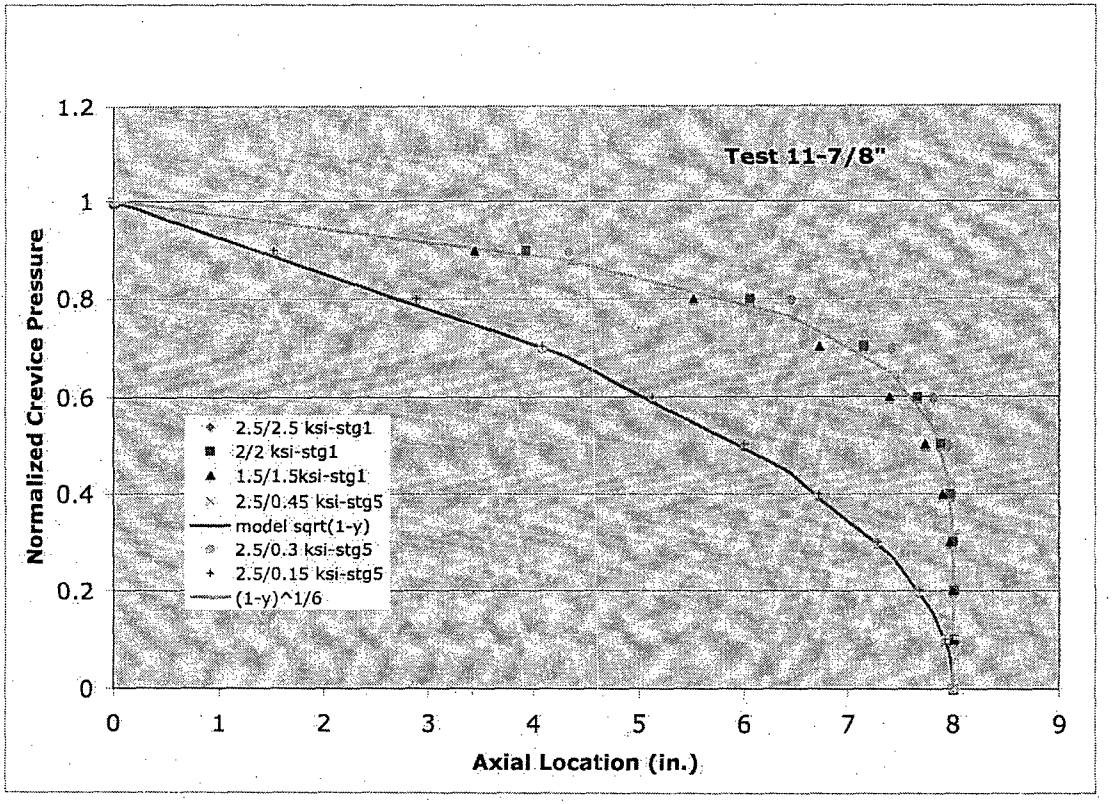


- Pressure distribution is parabolic when the gap is physically open.
- Pressure distribution is relatively uniform as long as contact is closed with positive contact pressure.

# Predicted vs. Observed Leak Rate (Test 01-3/4")

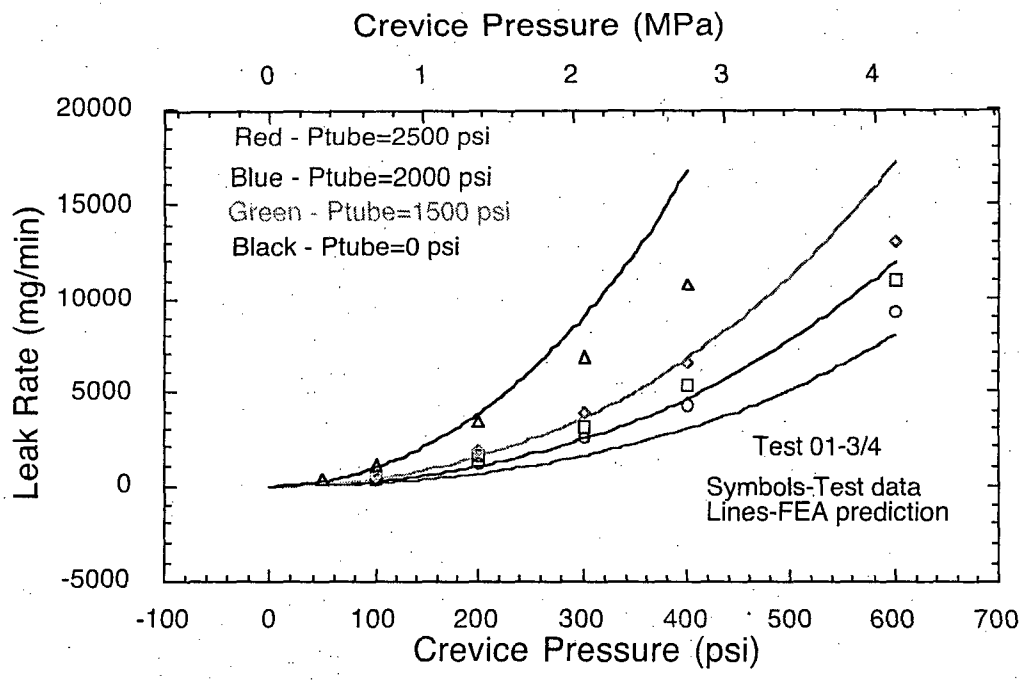


- 4" long specimen, crevice independently pressurized
- Specimen heated to 670°C, then tube pressurized to 2500 psi and held 4 h – no leakage.
- Then crevice was pressurized to 2000 psi and held for 4 h at 670°C – started leaking after 30 min.
- Final leak rate =8350 mg/min vs. predicted leak rate = 5500 mg/min.
- Specimen cooled to RT and leak tested.

# Predicted vs. Observed Leak Rate (Test 02-7/8")

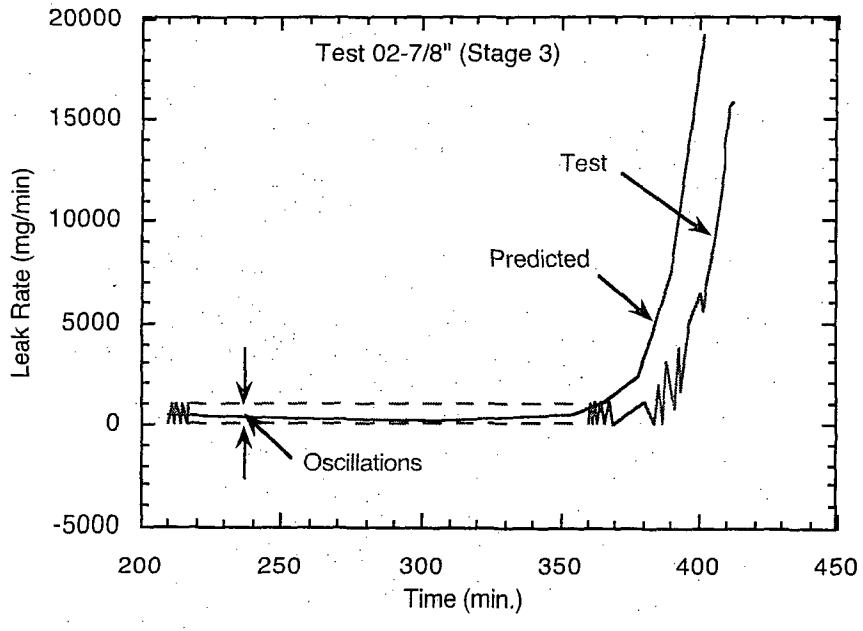


- Specimen 2" long, tube had a 1/32" dia. hole drilled in the tube wall.
- The inlet for crevice pressure was sealed off.
- Leak rate oscillation at low leak rate – not predicted, not observed when crevice is pressurized independently.
- Predicted leak rate based on crevice pressure = tube pressure.

# Leak Rate Analysis of Test 01-3/4"

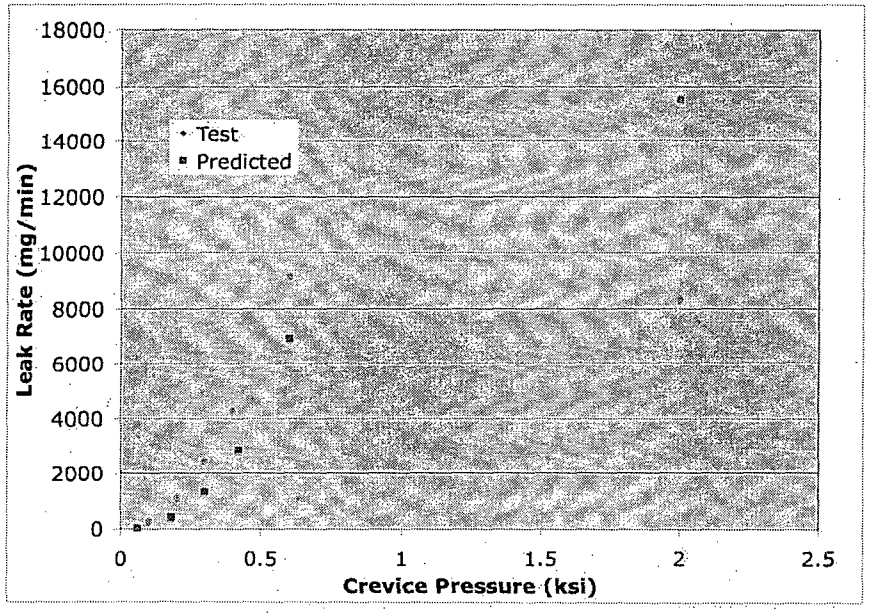


First approach

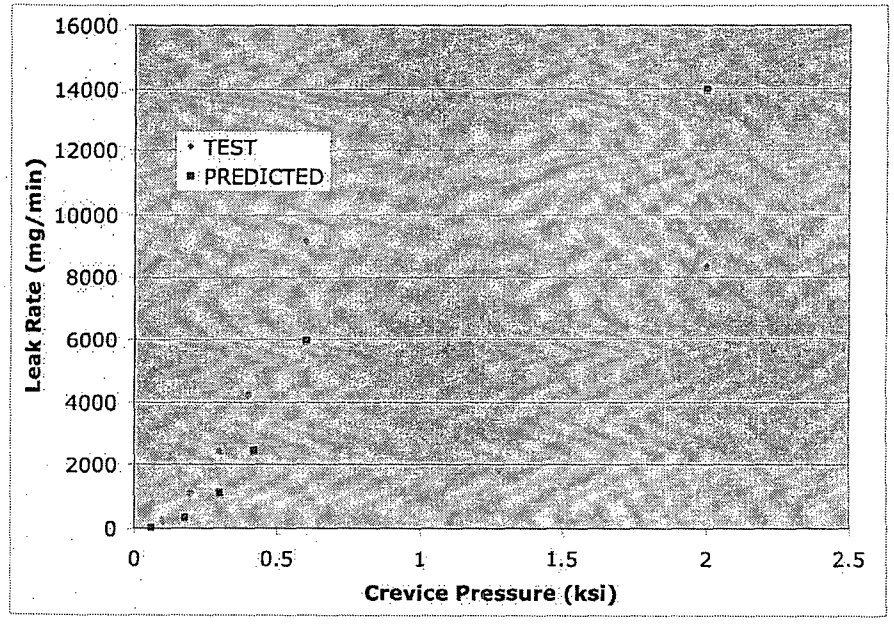


Second approach

- Leak rates predicted to within a factor of 2.
- We used the first approach to predict the leak rate of Model 51

# Leakage Analysis (Model 51)

- Contact pressures were calculated for uniform and parabolic crevice pressure distributions
- We assumed that the crevice pressure distribution for a physically open gap is parabolic for leakage analysis

$$\frac{p_f}{p_1} = \sqrt{1 - \left(\frac{z}{L}\right)}$$

- First, leak rate calculated with the same Eq. as the tube-to-collar specimens

$$q = \frac{-d^3}{12L}\frac{\rho_1}{\mu}\int_{p_1}^{p_2} \left(\rho(p_f)/\rho_1\right) dp_f = \frac{-d^3}{12L\nu_1 p_1}\int_{p_1}^{p_2} p_f dp_f$$

- The second approach was to use the basic equation for leak rate.

$$q = -\frac{\Delta p_f}{\int_0^L \frac{K\mu}{\rho} dz}$$

# Predicted Leak Rates for Model 51

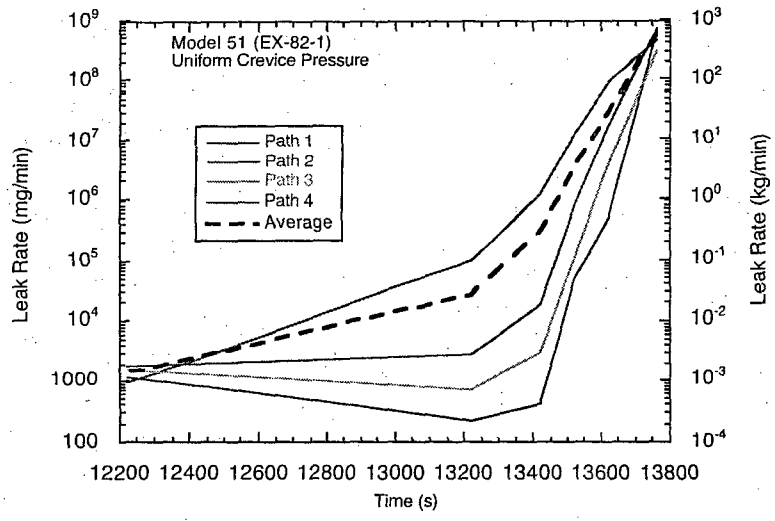


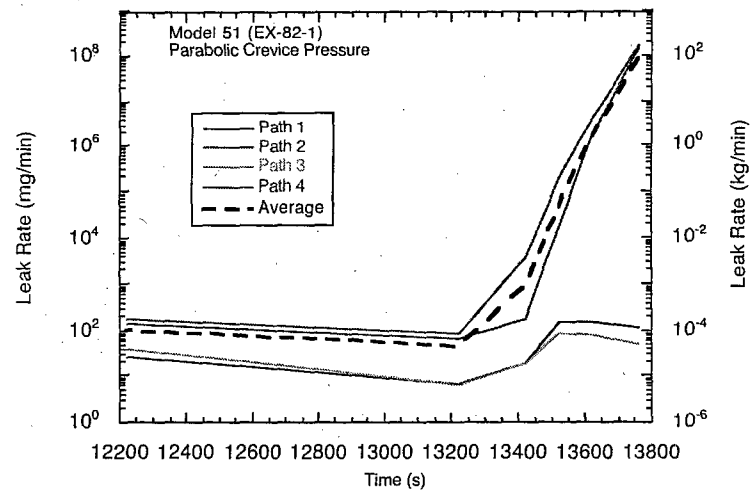

# Conclusions

- The leak rate tests showed that during high temperature ramp under both tube and crevice pressure, the leak rate remains very low until ~ 670-700°C, beyond which it increases rapidly with temperature
  - No large leakage observed if crevice was unpressurized.
  - Specimens with 0.75" diameter tube behaved essentially in the same fashion as specimens with 0.875" diameter tube.
  - High temperature leak rates were essentially the same for three heats of Alloy 600
- A test, in which the crevice pressure inlet was sealed off and a 1/32" hole was drilled in the tube wall, behaved essentially the same way as specimens whose crevices were independently pressurized.
  - If a throughwall crack is present in a tube within the tubesheet, the crevice will very likely be pressurized.
- A leak rate model was developed for axisymmetric contact pressure and gap opening
  - The predicted leak rates are within a factor of 2-3 of the observed leak rates in the tube-to-collar specimens.

# Conclusions – Cont'd

- A finite element model was developed for a Model 51 SG tube-to-tubesheet interface, including the tubesheet, tube, divider plate, SG shell and lower head.
  - Equivalent thermal and mechanical properties were developed for the tubesheet
    - *Limited high temperature tensile and creep tests were conducted on a heat of A508 steel and three heats of Alloy 600*
  - The heat loading on a single tube under consideration was modeled in a detailed fashion based on CFD input.
  - The heat loading on the rest of the tubes were smeared out over the tubesheet as volumetric heat flux.
- Stress analysis showed a significant variation in contact pressure and gap in the circumferential direction suggesting that circumferential flow will occur
  - The leak rate model predicted leak rates that were dependent on the location of the axial path around the circumference of the tube
  - The path-averaged leak rate is predicted to remain low ($<10^{-3}$ kg/min) until 13,400 s, then rising rapidly with time.
  - At 13,600 s, it is predicted to be within 5 and 10 kg/min.

## *Conclusions – Cont'd*

- In the absence of tests with realistic boundary conditions, these results should be considered as best estimates.

# *Uncertainties*

- How long does it take the crevice to be pressurized by leakage from the tube through a crack within the tubesheet?
- Are the contact pressures and gaps under the two types of bending of the tubesheet during the severe accidents captured in the FEM with sufficient accuracy?
- How would the circumferential flow affect the total leak rate?
- How sensitive is the calculated leak rate to material property variation?
- How sensitive is the leak rate to the thermal hydraulic uncertainties?

# *Leak Rate for Two Phase Flow (No Tubesheet Bowing)*

- Ring-Assembly Model (uniaxial stress field)

$$q = -\frac{1}{v_\ell L_\ell}\int_{p_1}^{p_{sat}} \frac{dp_f}{K}$$ in the liquid phase (incompressible) and

$$q = -\frac{1}{v_{sat} L_g}\int_{p_{sat}}^{p_2} \frac{p_f}{p_{sat}}\frac{dp_f}{K}$$ in the gas phase (ideal gas) with $L_g+L_l=L$

- FEA model (triaxial stress field)

$$q = -\frac{\Delta p_f}{\int_0^L \frac{K\mu}{\rho}dz}$$. However, K(z), i.e. $p_f(z)$ is apriori unknown

  - Use iterative solution

# *Iterative Solution Steps*

- Start with loss coefficients K(z) and contact pressures $p_f(z)$ as determined by the ring assembly model
- Perform FEA to determine new K(z)
- Calculate q
- Integrate $q = -\frac{1}{K}\frac{\rho(p_f)}{\mu}\frac{dp_f}{dz}$ from inlet to z to obtain next estimate of $p_f(z)$
- Iterate on $p_f$ (steps 3 and 4) until convergence
- Repeat Step 2 through Step 5 until convergence

# Results for Crevice Pressure Distribution at End of Iteration

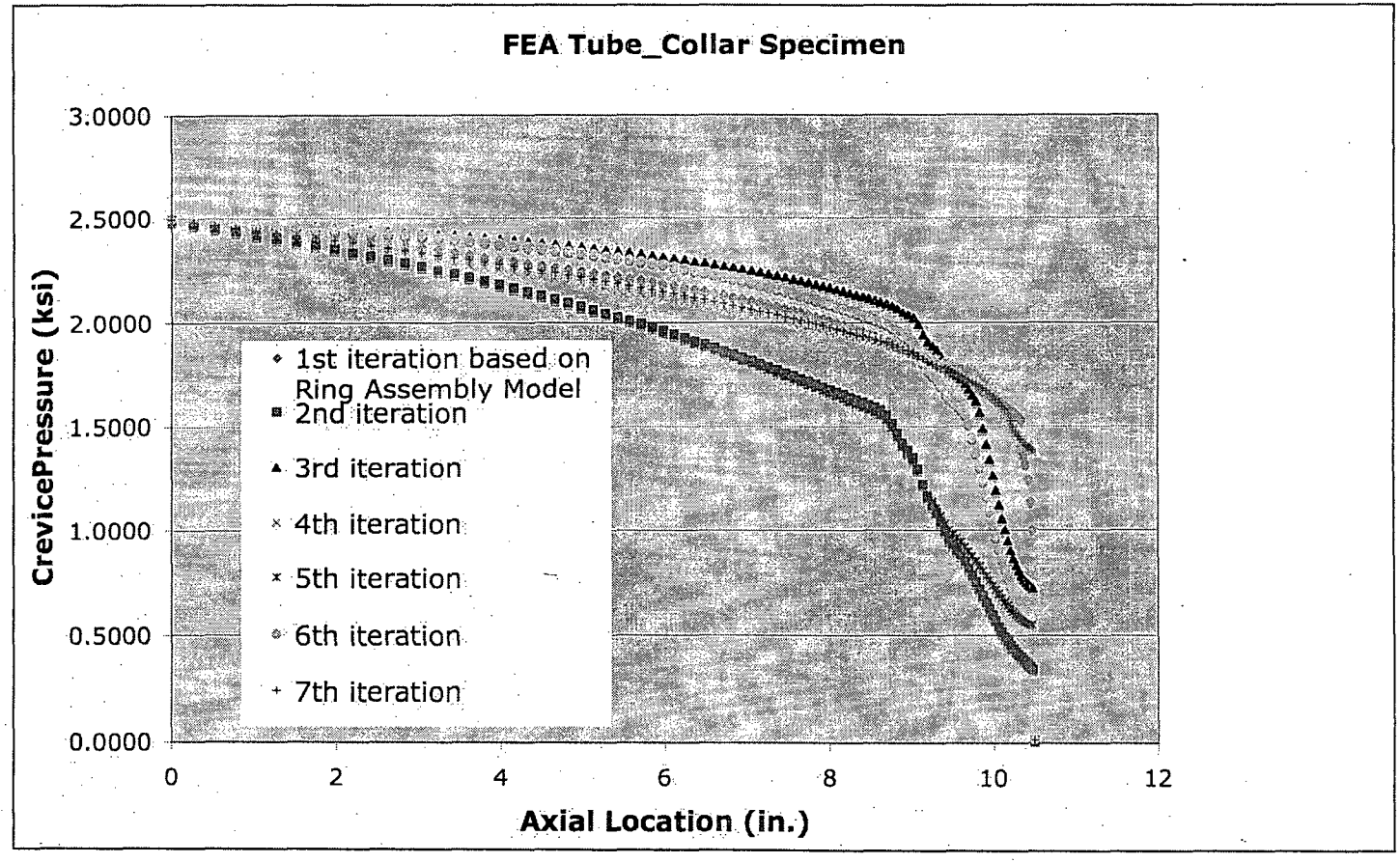


- Leak rate is 20 mg/min for higher crevice pressures and 8 mg/min for lower crevice pressures

# Results for Contact Pressures at Start of Iteration

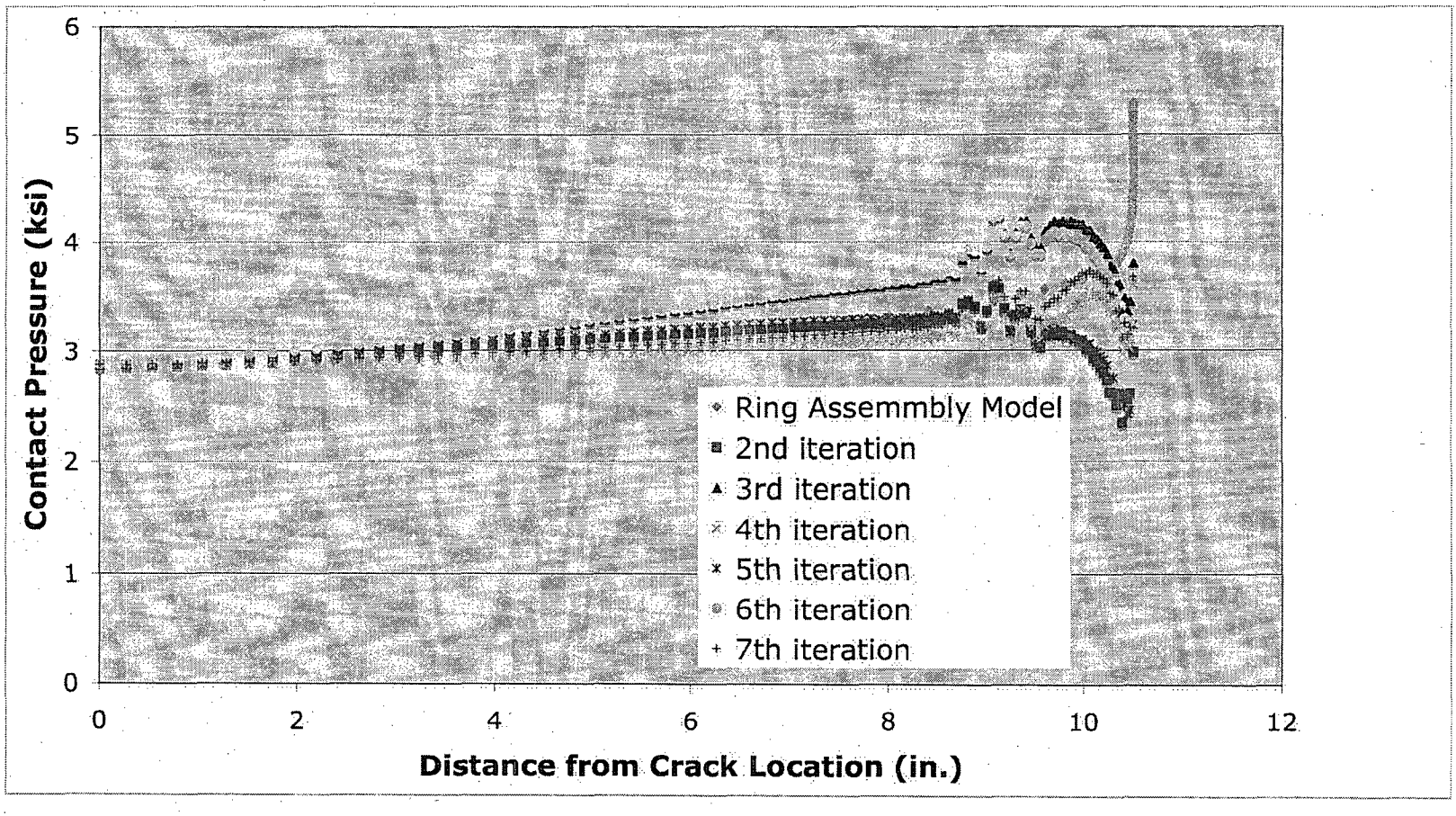

# Results for Leak Rate

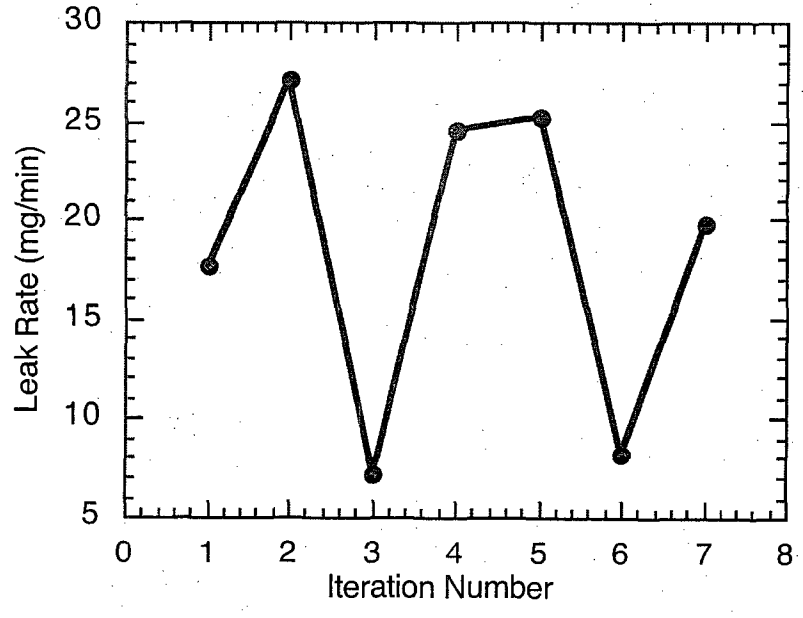


- Leak rate oscillates between 8 and 25 mg/min.
- Need to use a better iteration scheme.

# MSLB of Model 51 Including Tubesheet Bowing

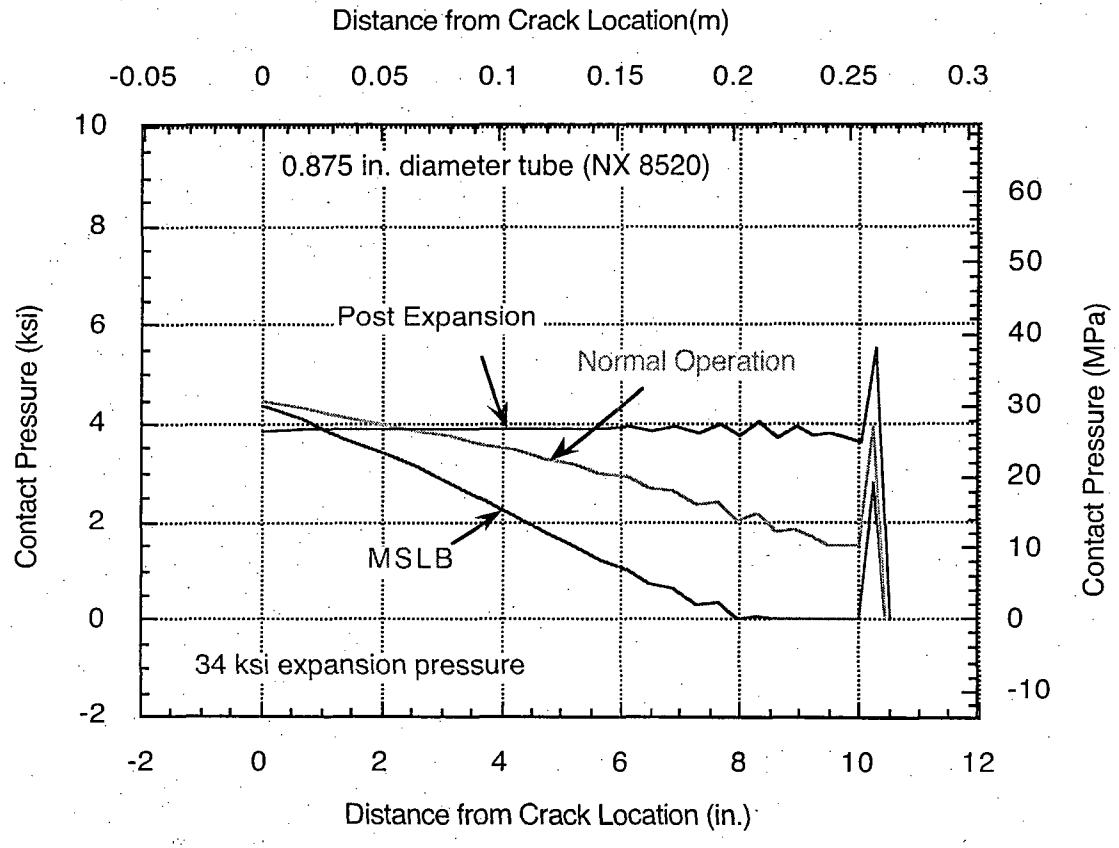


- Top 2.5" of interface loses contact during MSLB
- Iteration 1 calculation using Pcrev from ring assembly model shows a leak rate of 6.1 mg/min during NO and 16.5 mg/min during MSLB.
- More iterations are needed.

# Trends Observed in Tests Conducted to Date

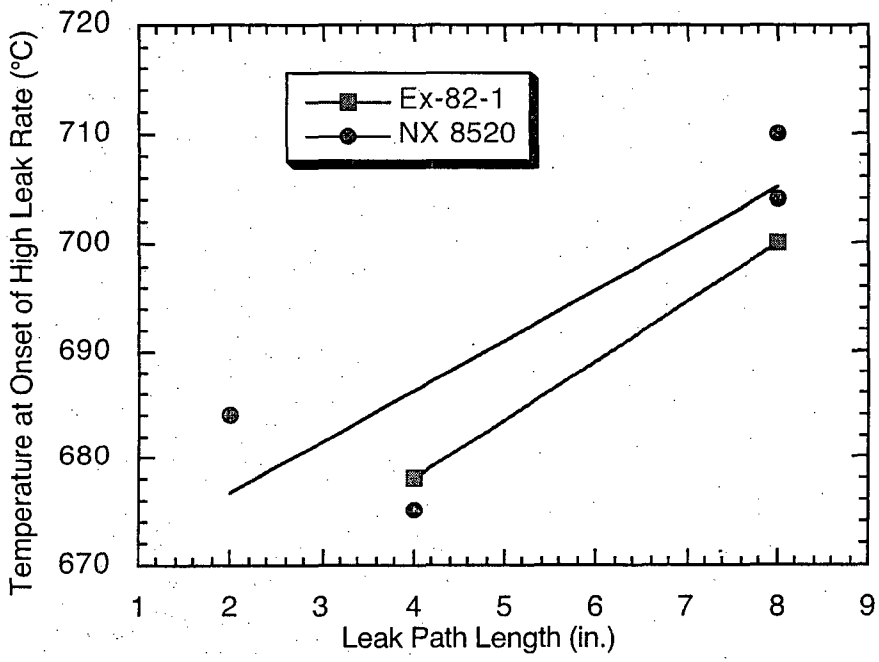


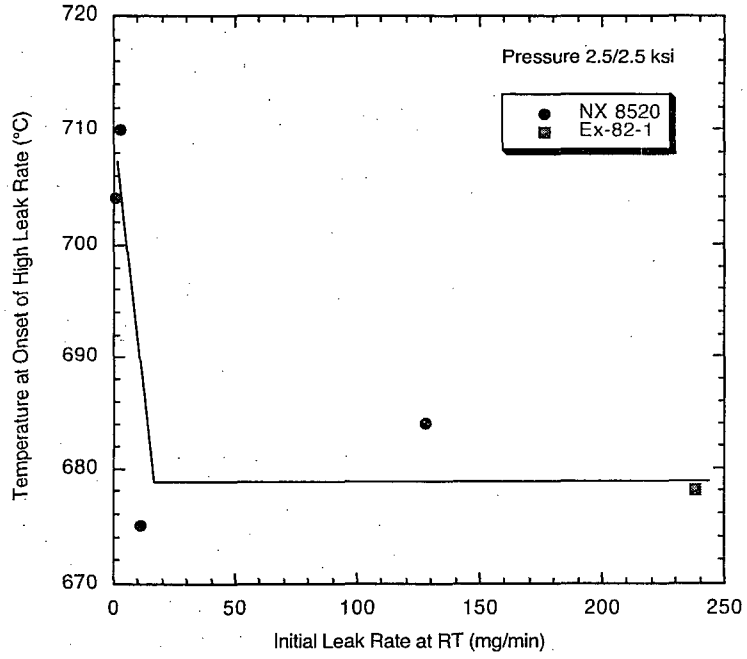


- Temperature at onset of high leakage increases with increasing leakage path length
- Temperature at onset of high leakage decreases with increasing initial leak rate at room temperature ("looser" joint)
  - It is independent of initial leak rate for high initial leak rate.